[21] Jin W, Yun C, Kwak MK, Kim TA, Kim SJ. TrkC binds to the type II TGF-beta receptor to suppress TGF-beta signaling. Oncogene 2007;26:7684-91.
[22] Sasahira T, Ueda N, Yamamoto K, et al. Trks are novel oncogenes involved in the induction of neovascularization, tumor progression, and nodal metastasis in oral squamous cell carcinoma. Clin Exp Metastasis 2012, in press.
[23] Sasahira T, Kirita T, Bhawal UK, et al. Receptor for advanced glycation end products (RAGE) is important in the prediction of recurrence in human oral squamous cell carcinoma. Histopathology 2007;51:166-72.
[24] Sasahira T, Kirita T, Kurihara M, et al. MIA-dependent angiogenesis and lymphangiogenesis are closely associated with progression, nodal metastasis and poor prognosis in tongue squamous cell carcinoma. Eur J Cancer 2010;46:2285-94.
[25] Allred DC, Harvey JM, Berardo M, Clark GM. Prognostic and predictive factors in breast cancer by immunohistochemical analysis. Mod Pathol 1998;11:155-68.
[26] Sasahira T, Kirita T, Oue N, et al. High mobility group box-1-inducible melanoma inhibitory activity is associated with nodal metastasis and lymphangiogenesis in oral squamous cell carcinoma. Cancer Sci 2008;99:1806-12.
[27] Martelli AM, Evangelisti C, Chiarini F, Grimaldi C, Manzoli L, McCubrey JA. Targeting the PI3K/AKT/mTOR signaling network in acute myelogenous leukemia. Expert Opin Investig Drugs 2009;18: 1333-49.
[28] Tessarollo L. Pleiotropic functions of neurotrophins in development. Cytokine Growth Factor Rev 1998;9:125-37.
[29] Sasahira T, Akama Y, Fujii K, Kuniyasu H. Expression of receptor for advanced glycation end products and HMGB1/amphoterin in colorectal adenomas. Virchows Arch 2005;446:411-5.
[30] Chen-Tsai CP, Colome-Grimmer M, Wagner Jr RF. Correlations among neural cell adhesion molecule, nerve growth factor, and its receptors, TrkA, TrkB, TrkC, and p75, in perineural invasion by basal cell and cutaneous squamous cell carcinomas. Deramatol Surg 2004;30:1009-16.
[31] Elliott RL, Blobe GC. Role of transforming growth factor beta in human cancer. J Clin Oncol 2005;23:2078-93.
[32] Le Scolan E, Zhu Q, Wang L, et al. Transforming growth factor-beta suppresses the ability of Ski to inhibit tumor metastasis by inducing its degradation. Cancer Res 2008;68:3277-85.
[33] Wang J, Yang L, Yang J, et al. Transforming growth factor beta induces apoptosis through repressing the phosphoinositide 3-kinase/AKT/survivin pathway in colon cancer cells. Cancer Res 2008;68:3152-60.
[34] Schroy P, Rifkin J, Coffey RJ, Winawer S, Friedman E. Role of transforming growth factor beta 1 induction of colon carcinoma differentiation by hexamethylene bisacetamide. Cancer Res 1990;50: 261-5.
[35] Langenskiöld M, Holmdahl L, Falk P, Angenete E, Ivarsson ML. Increased TGF-beta 1 protein expression in patients with advanced colorectal cancer. J Surg Oncol 2008;97:409-15.

AUTHOR QUERY FORM

ELSEVIER	**Journal: YHUPA** **Article Number: 2794**	**Please e-mail or fax your responses and any corrections to:** **Jill Shepherd** **E-mail: J.Shepherd@Elsevier.com** **Tel: 352-483-8113** **Fax: 352-483-3417**

Dear Author,

Please check your proof carefully and mark all corrections at the appropriate place in the proof (e.g., by using on-screen annotation in the PDF file) or compile them in a separate list. Note: if you opt to annotate the file with software other than Adobe Reader then please also highlight the appropriate place in the PDF file. To ensure fast publication of your paper please return your corrections within 48 hours.

For correction or revision of any artwork, please consult http://www.elsevier.com/artworkinstructions.

Any queries or remarks that have arisen during the processing of your manuscript are listed below and highlighted by flags in the proof. Click on the 'Q' link to go to the location in the proof.

Location in article	Query / Remark: click on the Q link to go Please insert your reply or correction at the corresponding line in the proof
Q1	Please confirm that given names and surnames have been identified correctly.
Q2	Please provide the academic degrees of all authors.
Q3	Please provide postal code.
Q4	Please spell out GAPDH.

Please check this box if you have no corrections to make to the PDF file. ☐

Thank you for your assistance.

ELSEVIER

Institut Pasteur

Microbes and Infection 15 (2013) 45–55

www.elsevier.com/locate/micinf

Original article

Selective estrogen receptor modulators inhibit hepatitis C virus infection at multiple steps of the virus life cycle

Yuko Murakami [a,*], Masayoshi Fukasawa [b], Yukihiro Kaneko [a], Tetsuro Suzuki [c,1], Takaji Wakita [c], Hidesuke Fukazawa [a]

[a] *Department of Bioactive Molecules, National Institute of Infectious Diseases, Toyama 1-23-1, Shinjuku-ku, Tokyo 162-8640, Japan*
[b] *Department of Biochemistry and Cell Biology, National Institute of Infectious Diseases, Tokyo, Japan*
[c] *Department of Virology II, National Institute of Infectious Diseases, Tokyo, Japan*

Received 15 June 2012; accepted 13 October 2012
Available online 23 October 2012

Abstract

We screened for hepatitis C virus (HCV) inhibitors using the JFH-1 viral culture system and found that selective estrogen receptor modulators (SERMs), such as tamoxifen, clomifene, raloxifene, and other estrogen receptor α (ERα) antagonists, inhibited HCV infection. Treatment with SERMs for the first 2 h and treatment 2–24 h after viral inoculation reduced the production of HCV RNA. Treating persistently JFH-1 infected cells with SERMs resulted in a preferential inhibition of extracellular HCV RNA compared to intracellular HCV RNA. When we treated two subgenomic replicon cells, which harbor HCV genome genotype 2a (JFH-1) or genotype 1b, SERMs reduced HCV genome copies and viral protein NS5A. SERMs inhibited the entry of HCV pseudo-particle (HCVpp) genotypes 1a, 1b, 2a, 2b and 4 but did not inhibit vesicular stomatitis virus (VSV) entry. Further experiment using HCVpp indicated that tamoxifen affected both viral binding to cell and post-binding events including endocytosis. Taken together, SERMs seemed to target multiple steps of HCV viral life cycle: attachment, entry, replication, and post replication events. SERMs may be potential candidates for the treatment of HCV infection.

Keywords: HCV; Tamoxifen; SERM (Selective estrogen receptor modulator)

1. Introduction

Over 170 million people in the world are infected with the hepatitis C virus (HCV). Approximately 20% of infected patients develop cirrhosis and hepatocellular carcinoma after chronic HCV infection. No HCV vaccine is available yet, and the current standard of care, which consists of a combination of interferon (IFN) and ribavirin, is only effective for approximately 50% of infected patients, and many patients have serious side effects. Because of the urgent need for novel HCV therapeutics, research is being conducted to develop new anti-HCV drugs. In addition to *in vitro* screening assays that target HCV-specific enzymes, other approaches that use replicon cells and the recently described Huh 7.5.1-JFH-1 (genotype 2a)-infection system have been developed [1]. The Huh 7.5.1-JFH-1-infection system is an excellent system to identify HCV inhibitors that interfere with individual steps of the HCV life cycle, such as viral attachment, entry, and release. This experimental system allows both viral and host components that are involved in HCV infection to be targeted. Although drugs that target the host components may be toxic, such drugs are unlikely to select for resistant viruses.

We screened chemicals using a cell-based screening system [2] and found that tamoxifen and other selective estrogen receptor modulators (SERMs) inhibited HCV infection. Tamoxifen has been successfully used for the treatment of breast cancer since it was found to be an ER antagonist over 30 years ago. Clomifene and raloxifene, which are compounds

* Corresponding author. Tel.: +81 3 5285 1111x2327; fax: +81 3 5285 1272.
E-mail address: murakami@nih.go.jp (Y. Murakami).
[1] Present address: Department of Infectious Diseases, Hamamatsu University School of Medicine, Hamamatsu, Japan.

1286-4579/$ - see front matter © 2012 Institut Pasteur. Published by Elsevier Masson SAS. All rights reserved.
http://dx.doi.org/10.1016/j.micinf.2012.10.003

that are related to tamoxifen, have been developed and used for the treatment of breast cancer and for the treatment of anovulation and osteoporosis. Currently, these three SERMs and toremifene have been approved in Japan and the US, and next-generation SERMs are undergoing clinical evaluation.

Because tamoxifen exhibited the ability to inhibit HCV infection, we determined which SERMs could effectively inhibit HCV infection and be approved for clinical use. The first-generation SERMs—tamoxifen, clomifene, and raloxifene—were all effective against HCV as were other ERα antagonists. We examined whether SERMs could be utilized as new drugs for the treatment of HCV.

2. Materials and methods

2.1. Cells and virus

Human hepatoma cell line, Huh 7.5.1 cells and human embryonic kidney 293T cells were cultured in Dulbecco's modified Eagle's medium (DMEM) (Sigma–Aldrich Co. St. Louis, MO, USA) with 10% fetal bovine serum (FBS). HCV-JFH-1 (HCVcc) (genotype 2a) was the culture supernatant of infected Huh 7.5.1 cells as described previously [2]. A subgenomic replicon cell line, clone #4-1, which harbors the genotype 2a (JFH-1) [3,4], and clone #5-15, that harbors the genotype 1b HCV genome [5], were also cultured in DMEM with FBS.

2.2. Chemicals

The SCADS inhibitor kit I was provided by the Screening Committee of Anticancer Drugs, supported by a Grant-in-Aid for Scientific Research on the Priority Area "Cancer" from The Ministry of Education, Culture, Sports, Science and Technology of Japan. Tamoxifen, diethylstilbestrol, triphenylethylene, 17β-estradiol, and brefeldin A were purchased from Sigma–Aldrich Co. (St. Louis, MO, USA). Clomifene was purchased from LKT Laboratories, Inc. (St. Paul, MN, USA), and hydroxytamoxifen ((*z*)-4-hydroxytamoxifen) and raloxifene were purchased from Enzo Life Sciences, Inc. (Farmingdale, NY, USA). Chloroquine was purchased from WAKO (Osaka, Japan). Other chemicals were purchased from Tocris Bioscience (Bristol, UK).

2.3. Quantification of the viral titer in medium

Huh 7.5.1 cells were seeded in 96-well plates at a density of 2×10^4 cells per well in a volume of 120 μl. The next day, 15 μl of media that contained the test compound and 15 μl of the HCVcc virus stock solution at a moi of 0.01 were added to each well. After 5 days, 100 μl of the culture supernatant was taken from each well, and viral RNA was extracted. Total RNA was also extracted from the cells. Quantitative real-time RT-PCR was then performed with One step SYBR PrimeScript RT-PCR Kit (Takara-Bio Co., Otsu, Japan) as described previously [2]. In the case of #4-1 replicon cell, as an internal control, glyceraldehyde-3-phosphate dehydrogenase (GAPDH) were measured with primers 5′-CCACCCATGGCAAATTCC-3′ and 5′-TGGGATTTCCATTGAT-3′. Cell growth was monitored using the MTT assay as described previously [6].

2.4. Western blotting

Western blotting was performed as previously described [2]. Briefly, cell lysates that contained equal quantities of protein were separated by SDS-PAGE, transferred onto PVDF membranes, and probed with antibodies against the core antigen (2H9), NS5A (Austral Biologicals, San Raman, CA, USA), or GAPDH (Santa Cruz Biotech. Inc., Santa Cruz, USA). After incubation with horseradish peroxidase-conjugated secondary antibodies, the protein bands on the PVDF membranes were detected using an ECL system (GE Healthcare UK Ltd., Amersham Place, UK).

2.5. Production of and infection with pseudo-particles

HCV pseudo-particles (HCVpp) were generated using the following 3 plasmids: a Gag-Pol packaging construct (Gag-Pol 5349), a transfer vector construct (Luc 126), and a glycoprotein-expressing construct (HCV E1E2) (JFH-1, 2a). The generation of the pseudo-particles was performed according to the method described by Bartosch et al. [7]. To express the glycoproteins of other HCV genotypes, HCV E1E2 constructs of the genotypes 1a (H77), 1b (UKN1B 12.6), 2b (UKN2B 2.8), and 4 (UKN4 11.1) were generously provided by Dr. F. Cosset (INSERM, France) [8]. To produce VSVpp, a plasmid that coded the vesicular stomatitis virus (VSV) envelope, pCAG-VSV, was generously provided by Dr. Y. Matsuura (Osaka University, Japan). Gag-Pol 5349 (3.1 μg), Luc 126 (3.1 μg), and each of the individual glycoprotein-expression constructs (1.0 μg) were co-transfected into 293T cells that were seeded on a 10-cm dish (2.5×10^6 cells) using TransIT-LT1 Transfection Reagent (21.6 μl) (Mirus Bio LLC, Madison, WI, USA). The medium from the transfected cell cultures was harvested and used as the pseudo-particle stock. For the infection assay, Huh 7.5.1 cells were seeded onto a 48-well plate at a density of 4×10^4 cells per well one day prior to infection. The medium was then removed, and the cells were subsequently infected with the pseudo-particles in the presence or absence of drug. The cells were then incubated for 3 h. The VSVpp preparation was diluted (1:600) to infect with similar RLU activity compared to the HCVpp. The supernatant was then removed, fresh culture medium was added to the cells, and the cells were incubated for an additional 3 days. The luciferase assays were performed using a luciferase assay system (Promega Co. Madison WI, USA). Anti-CD81 antibody (sc-23962) was purchased from Santa Cruz Biotech.

3. Results

3.1. Tamoxifen and estrogen receptor α antagonists inhibited HCV infection

Using quantitative RT-PCR, we screened the compounds in the SCADS inhibitor kit I. Drugs and HCVcc at a moi of 0.01

were added to Huh 7.5.1 cells. Five days later, the quantity of HCV RNA in the culture supernatant was measured using quantitative real-time RT-PCR [2]. We found that tamoxifen reduced the levels of JFH-1 RNA in the culture supernatant. We also examined the effects of other SERMs and agonists and antagonists of ERα. As shown in Fig. 1, tamoxifen, clomifene, and hydroxytamoxifen, which have a triphenylethylene backbone, exhibited intense inhibitory effects (EC_{50}: approximately 0.1 μM). Triphenylethylene showed reduced inhibitory activity (data not shown). Raloxifene also inhibited viral RNA production at a similar concentration. (EC_{50}: approximately 0.1 μM) (Fig. 1a). Tamoxifen and raloxifene display both ERα antagonist and agonist properties in a dose- and tissue-dependent manner [9]. In contrast, ICI 182,780 (fulvestrant), ZK164015, and MPP (methyl-piperidino-pyrazole) are exclusively antagonistic [10–12]. These ERα antagonists also showed inhibitory activity against JFH-1, but their EC_{50} values were approximately 1 μM (Fig. 1b). As the 50% toxic concentrations (TC_{50}) for these compounds were observed to be greater than 10 μM (Fig. 1a and b), these specific indexes are over 100. In contrast, the ERα agonists 17β-estradiol, diethylstilbestrol, and PPT (1,3,5-tris(4-hydroxyphenyl)-4-propyl-1*H*-pyrozole) did not inhibit HCV (Fig. 1c). As expected, the SERMs that were observed to effectively inhibit HCV RNA production also reduced the core protein levels intracellularly (Fig. 1d).

3.2. SERMs inhibited more than one step of the JFH-1 life cycle

To determine which step of the JFH-1 life cycle was inhibited by the SERMs studied, we performed time-of-addition experiments. As described previously [2], JFH-1 appears to complete one infectious life cycle in approximately 48 h. Huh 7.5.1 cells were inoculated with JFH-1-containing medium (moi 0.1) with or without drug and were then incubated for 2 h. After the medium was removed, fresh medium with or without drug was added. The cells were then incubated for another 46 h. Treatment with 10 μM tamoxifen for 48 h reduced the amount of viral RNA in the medium to 1.7% of levels observed in the control. Treatment with tamoxifen for the first 2 h after infection (0–2 h) reduced viral RNA to 2.3% of the levels observed in the control. The addition of tamoxifen to the fresh medium just after the removal of the virus (2–48 h) resulted in a reduction in the amount of viral RNA to 10.7% of the levels observed in the control. The addition of tamoxifen 24 h after viral inoculation (24–48 h) resulted in a decrease in the amount of viral RNA to 60% of the levels observed in the control (Fig. 2a). This result suggests that tamoxifen inhibits mainly viral entry and some steps during replication. 10 μM of raloxifene exhibited a similar inhibitory pattern but less inhibited by the treatment after the entry step (Fig. 2b). A pure ERα antagonist, ICI 182,780 (30 μM), also exhibited inhibition of both viral entry and the replication steps, but the inhibition of the entry step was not so marked (Fig. 2c).

To further investigate effect on HCV post replication, we infected HCV in the presence of the drugs for 72 h (moi 0.1) and examined their effects on intracellular and extracellular HCV RNA levels. Brefeldin A, an inhibitor of protein transport [13], was used as a positive control of post replication inhibition. In this experimental setting, brefeldin A showed intracellular HCV RNA accumulation suggesting post replication inhibition (Fig. 2d). SERMs generally reduced HCV RNA in cell as well as HCV RNA in medium, although the extent of reduction was different (Fig. 2d). Lower concentration of SERMs reduced extracellular HCV RNA more robustly than intracellular HCV RNA. At a concentration of 0.1 μM, tamoxifen exclusively inhibited HCV RNA in the culture supernatant but not intracellular HCV RNA levels, in a manner similar to that of brefeldin A (Fig. 2d). The results suggest that SERMs inhibit post replication step(s) such as assembly or release. Because low concentrations of tamoxifen failed to inhibit intracellular HCV RNA, SERMs potentially target post replication step(s) more efficiently than replication step. In this condition, higher concentrations (1 and 3 μM) of tamoxifen seemed to inhibit intracellular HCV RNA rather than extracellular HCV RNA, although the reason is not clear.

To determine the effect of these drugs on chronic infection, we used pre-infected Huh 7.5.1 cells. We infected the cell with HCVcc at a moi of 0.01 and incubated for 3 days. Three days after infection, the drugs were added, and the cells were further incubated for 48 h. At the time of drug addition, the cells were persistently infected, and HCVcc was continuously produced and released into the culture supernatant, which is similar condition to chronic infection. HCV RNA was extracted from the culture supernatant and the cells after 48 h and measured copy number of HCV RNA. Both HCV RNA in the culture supernatant and that in the cell were reduced by treatment with the SERMs, but the intracellular HCV RNA levels were less reduced (Fig. 2e). This suggested that the SERMs caused preferential reduction in extracellular HCV RNA through interference with some post replication step(s), such as assembly or release. Brefeldin A accumulated intracellular HCV RNA, and reduced HCV RNA level in the culture supernatant (Fig. 2e).

These data suggested that the SERMs inhibit multiple steps in the HCV life cycle: entry, viral RNA replication and some post replication step(s).

3.3. SERMs inhibited copies and NS5A protein expression in replicon cells

To confirm the effect of these drugs on viral replication, we used two subgenomic replicon cells. The subgenomic replicon cells, derived from Huh7 cells, harbor HCV viral RNA that replicates autonomously, and they express viral proteins. We treated cells that harbored a subgenomic replicon (#4-1, genotype 2a) [3,4] with the SERMs for 48 h and measured the amount of cellular replicon RNA by quantitative RT-PCR. Treatment with 10 μM of tamoxifen, raloxifene, or 3 μM of clomifene, inhibited HCV RNA compare to GAPDH RNA, although statistical significance was shown in only the inhibition of 10 μM of tamoxifen. ICI 182,780 did not show specific inhibition of HCV RNA (Fig. 3a).

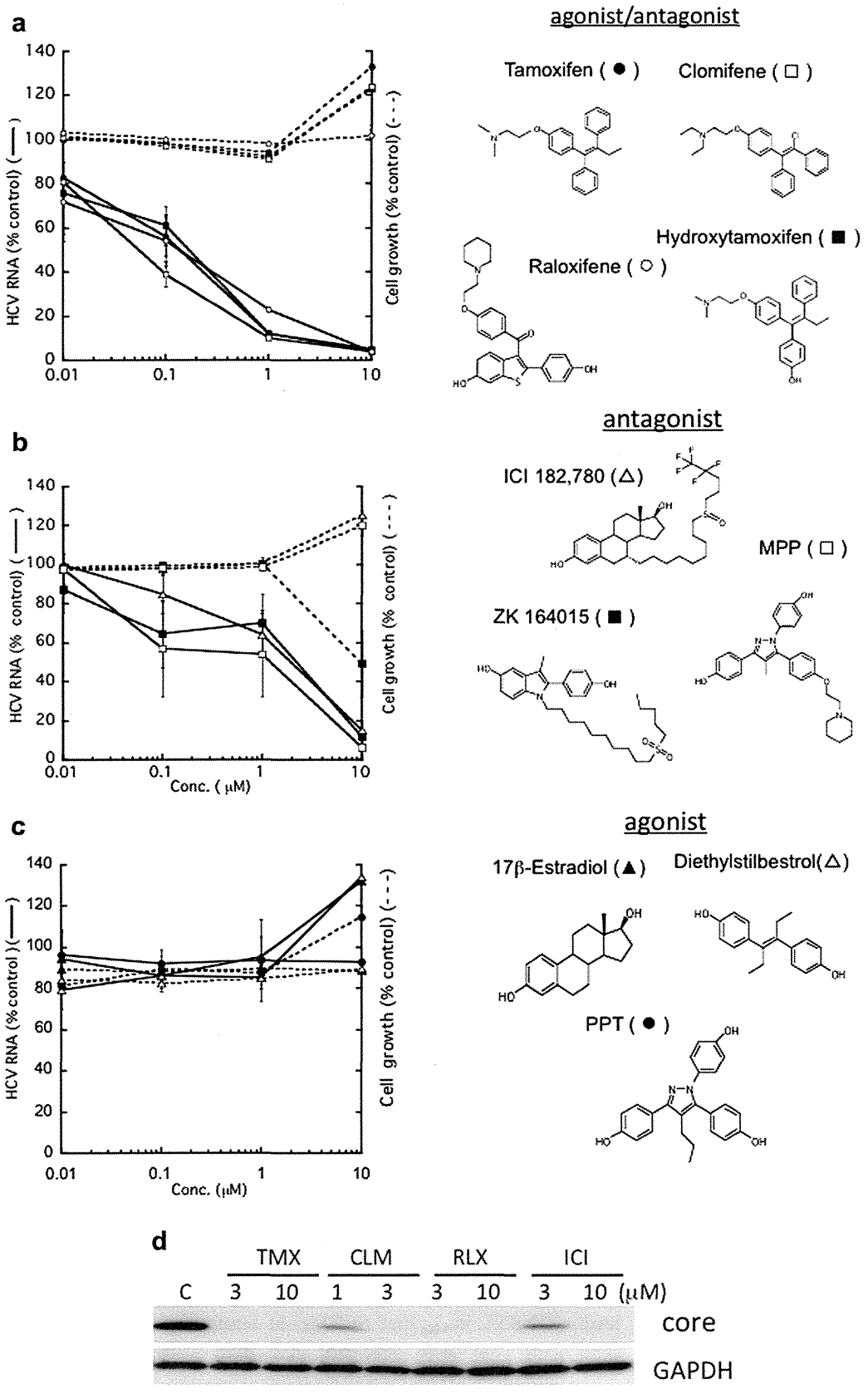

Fig. 1. Effects of SERMs on JFH-1 HCV RNA levels. a) Effects of tamoxifen, clomifene, and raloxifene. Huh 7.5.1 cells were infected with HCV JFH-1 (moi 0.01) in the presence of drugs and were incubated for 5 days. Drugs were added just before viral inoculation. HCV RNA in the medium was measured by tube-capture-RT-PCR [2]. Parallel cultures of cells without virus were analyzed using the MTT assay to detect the inhibition of cell growth due to drug exposure. Tamoxifen (closed circles), clomifene (open rectangles), hydroxytamoxifen (closed rectangles), and raloxifene (open circles). The percentages to control HCV RNA and

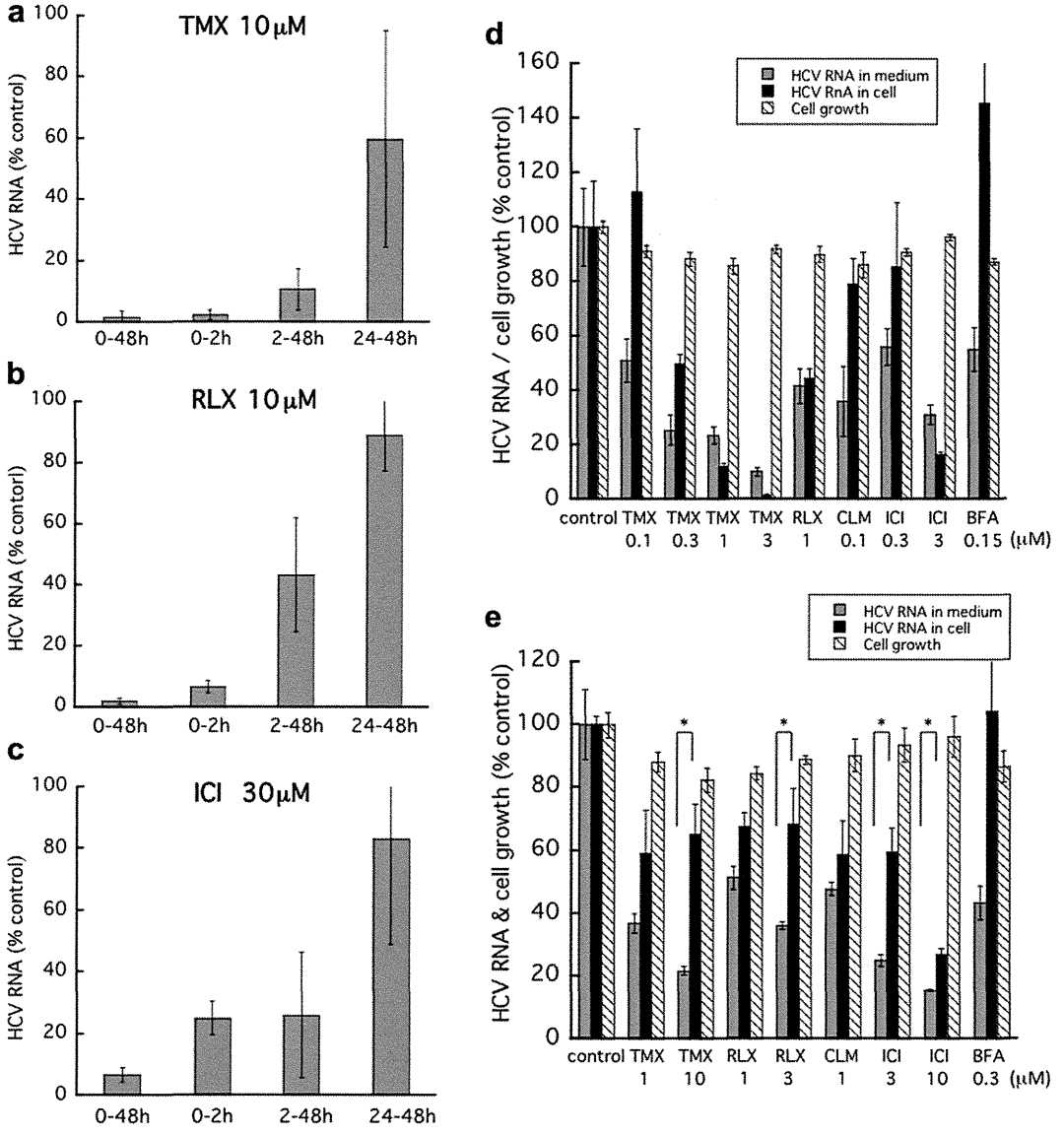

Fig. 2. Time-of-addition experiments (a–c) and the effect of SERMs on extracellular and intracellular HCV RNA in simultaneous infection (d) and in persistent infection (e). Huh 7.5.1 cells were treated with tamoxifen (TMX) (10 μM, a), raloxifene (RLX) (10 μM, b), or ICI 182,780 (ICI) (30 μM, c) during the following time periods: 0–2 h, 2–48 h, or 24–48 h after JFH-1 infection (moi 0.1). Forty-eight hours after infection, the culture supernatant was harvested, and HCV RNA was extracted and subjected to quantitative real-time RT-PCR to determine the number of copies of the JFH-1 genome. The data are the averages of three independent experiments and the standard deviation. d) Effect of treatment with SERMs for 3 days on extra- and intra-cellular HCV RNA levels. Huh 7.5.1 cells were infected with JFH-1 (moi 0.1) just after addition of the SERMs. Three days later, RNA was extracted from the cells and from the culture supernatant. The amount of HCV RNA was measured by quantitative real-time RT-PCR. Brefeldin A (BFA) was used as a positive control. e) Huh 7.5.1 cells were infected at a moi of 0.01, 3 days before addition of drugs. The infected cells were treated with SERMs for 48 h. RNA was subsequently extracted from the cells and the culture supernatant to determine the viral genome copy number. The results are presented as the percentage of control cells without drug. The data are the averages of triplicates and the error bars represent standard deviation. *P-value < 0.05. One representative experiment of two independent experiments is shown.

Next we treated this (#4-1, genotype 2a) and another replicon (#5-15, genotype 1b) [5] with the SERMs for 3 days and examined the effect of the compounds on the HCV NS5A protein levels by western blotting. As shown in Fig. 3b, the SERMs except ICI 182,780 reduced the level of NS5A in accordance with the results in Fig. 3a. ICI 182,780 seemed to slightly reduce NS5A protein in #5-15 replicon cell. The SERMs did not reduce the protein levels of GAPDH in the subgenomic replicon cells (Fig. 3b). These results indicated that SERMs, at least tamoxifen, raloxifene and clomifene,

control cell growth are indicated by solid lines and dotted lines, respectively. b) Effect of the following ERα antagonists: ICI 182,780 (closed triangles), ZK164015 (closed rectangles), and MPP (open rectangles). c) Effect of the following ERα agonists: 17β-estradiol (closed triangles), diethylstilbestrol (open rectangles), and PPT (closed circles). The results are presented as percentages of the control cells that were not treated with drugs. Values are the averages of triplicates, and the error bars represent the standard deviation of the mean. One representative experiment of three independent experiments is shown. d) Huh 7.5.1 cells were infected (moi 0.01) in the presence of tamoxifen (TMX), clomifene (CLM), raloxifene (RLX), or ICI 182,780 (ICI) and incubated for 5 days. Cell lysates were blotted with anti-core and anti-GAPDH antibodies as described in the Section Materials and methods.

were effective not only against HCV genotype 2a but also HCV genotype 1b and that the compounds inhibited a HCV replication step. The growth of the replicon cells was suppressed by treatment with 10 μM of clomifene. Clomifene at concentrations less than 10 μM and tamoxifen, raloxifene and ICI 182,780 at 10 μM concentration or lower did not inhibit cell growth (Fig. 3c).

3.4. SERMs inhibited entry of HCVpp but not VSVpp

To further examine the inhibition of early viral processes by the SERMs, we used infectious HCV pseudo-particles (HCVpp). Because HCVpp enter into cell dependent on HCV envelope protein but replicate dependent on retroviral system in the cell, we can exclude other effects of the drug except effect on HCV entry system. Pseudo-particles with the viral envelope glycoprotein mimic the entry of the parental virus, and this system has been used for investigation of HCV entry [7,8,18,20,21]. The infectious titer is determined by luciferase activity. We added tamoxifen to HCVpp- or VSVpp-containing medium and incubated Huh 7.5.1 cells with this medium for 3 h. After washing the cells, fresh medium was added, and the cells were incubated for 3 days. Treatment with tamoxifen reduced the luciferase activity of the cells that were infected with HCVpp in a dose-dependent fashion. In contrast, the luciferase activity caused by VSVpp was not reduced by the same concentrations of tamoxifen (Fig. 4a). We also examined the effect of other SERMs, such as clomifene, raloxifene, ICI 182,780, ZK164015, and MPP, on HCVpp infection. All of these SERMs inhibited the luciferase activity caused by HCVpp but not the activity caused by VSVpp (Fig. 4b). ICI 182,780 showed a weaker effect compared to tamoxifen, clomifene and raloxifene. Next, we examined the effects of these drugs on various genotypes of HCVpp. Although the extent of inhibition was varied, the compounds inhibited all of the genotypes that were examined (Fig. 4c). At a concentration of 10 μM, ICI 182,780 inhibited all of the genotypes of HCVpp other than genotype 2a. These results suggested that the SERMs inhibit entry of all genotypes of HCV.

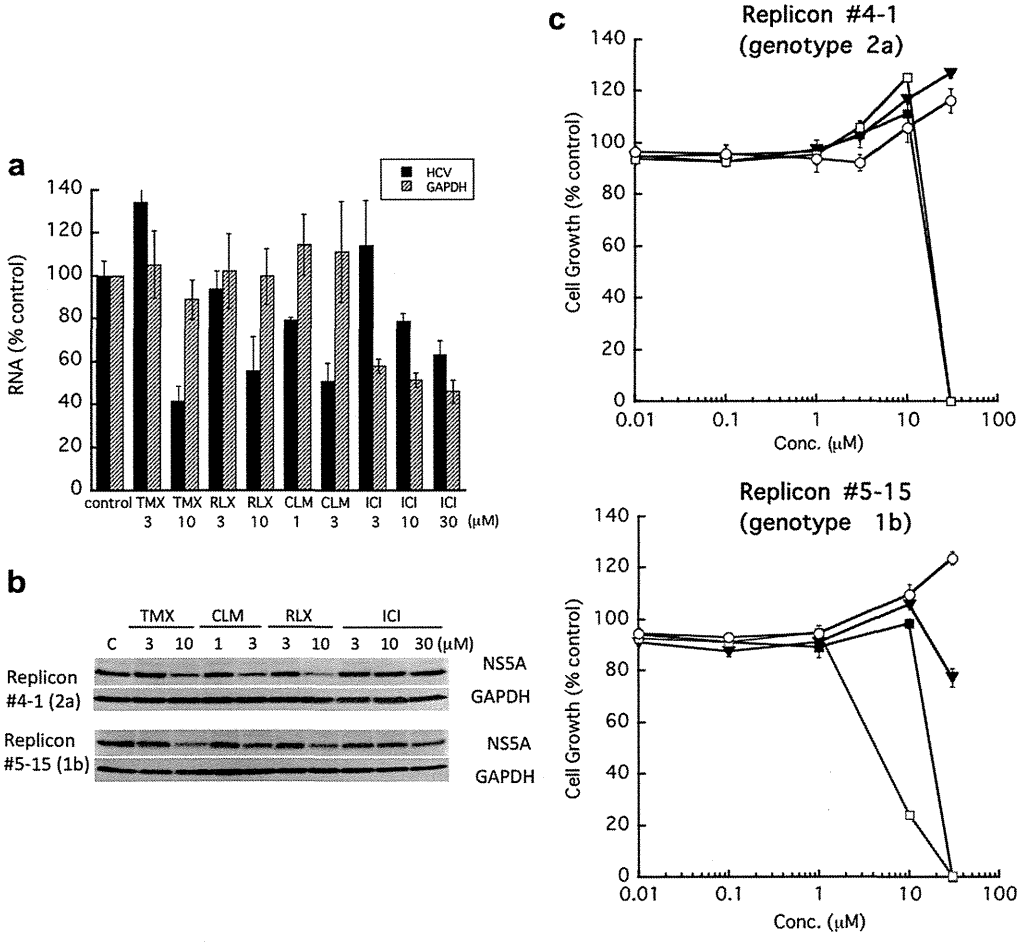

Fig. 3. The effect of SERMs on cells that harbored a subgenomic replicon. A subgenomic-replicon-harboring cell line clone #4-1 (genotype 2a) was treated with SERMs for 48 h. The total RNA was extracted from the cells, and amount of HCV RNA genome was measured. As an internal control, relative amount of GAPDH RNA was measured and indicated as percentage of control cells without drug (a). Another subgenomic-replicon-harboring cell line, clone #5-15 (genotype 1b) was treated with SERMs for 3 days. Cell lysates were subjected to western blotting with an anti-NS5A antibody or an anti-GAPDH antibody (b). Cells that were grown for 3 days in the presence of tamoxifen (closed rectangles), clomifene (open rectangles), raloxifene (closed triangles), or ICI 182,780 (open circles) were measured using the MTT assay. Cell growth is expressed as a percentage of control cells without drug (c). The values are the average of triplicate and the error bars represent the standard deviation of the mean. One representative experiment of two independent experiments is shown.

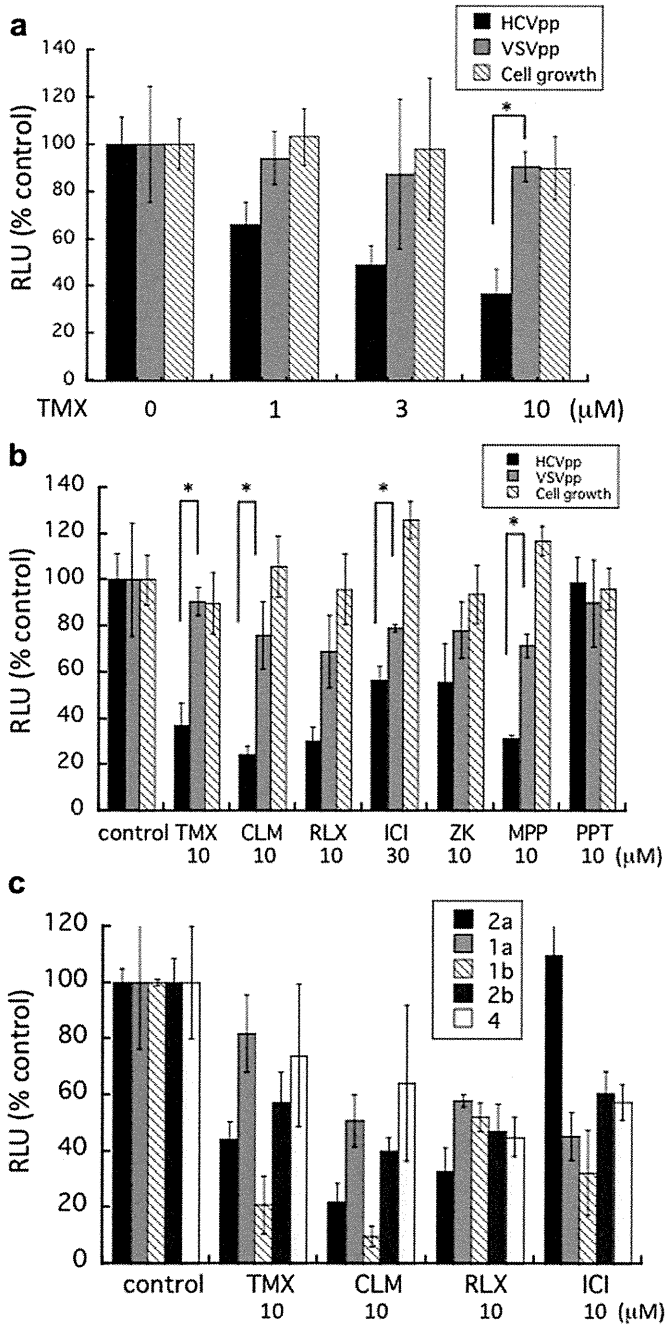

Fig. 4. Effect of SERMs on HCV pseudo-particle (HCVpp) infection. a) Huh 7.5.1 cells were incubated with pseudo-particles (HCVpp or VSVpp) in the presence or absence of tamoxifen for 3 h. The supernatants were removed, medium was added back to the cell cultures, and the cells were incubated for another 3 days. The VSVpp preparation was diluted 600 times so it was infected at similar RLU activity levels compared to HCVpp (approximately 5000 RLU). A parallel culture without pseudo-particles was analyzed using the MTT assay to evaluate the effect of the drugs on cell growth. b) Effects of various SERMs on HCVpp and VSVpp infection. c) Effects of SERMs on the various genotypes of HCVpp infection. The control luciferase activities were approximately 5000 RLU (genotype 2a), 3000 RLU (genotype 1a), 2400 RLU (genotype 1b), 3900 RLU (genotype 2b), and 860 RLU (genotype 4). The values are expressed as the percentage of control cells without drug. The data are the averages of three wells and the error bars are the standard deviation of the mean. *P-value < 0.05. One representative experiment of three independent experiments is shown.

3.5. Effect of tamoxifen on the attachment and entry steps

To better understand how tamoxifen blocks HCV entry, we performed an experiment to discriminate between the inhibition of HCV attachment to cells and the inhibition of post-binding entry events. HCV attaches to several cellular receptors via its E1 and E2 envelope proteins and enters via clathrin-mediated endocytosis [14–16]. We used HCVpp because infection with HCVpp is thought to simulate HCV entry [7,17,18] and the entry is independent of HCV replication. HCVpp binding to the cellular receptors was performed at 4 °C for 1.5 h. Under these conditions, HCVpp bind to the cells but entry is not efficient. The inoculum was removed, and fresh medium was added to the cells. The cells were subsequently incubated at 37 °C. In protocol I, the drug was administered during the binding step at 4 °C. After the shift to 37 °C, treatment with the drug was performed during first hour (protocol II) or after 1 h at 37 °C (protocol III) to distinguish between the inhibition of early and late post-binding events (Fig. 5a). The inoculum was removed after treatment, and fresh medium was added to the cells. We used chloroquine, a lysosome-tropic agent, as a control inhibitor for early entry (protocol II) [19]. We also used an anti-CD81 antibody that specifically inhibits HCV entry through the inhibition of the HCV cellular receptor protein CD81 at early entry [20,21]. As expected, chloroquine inhibited luciferase activity when the cells were treated during the early post-binding step (protocol II). This result suggested that endocytosis occurred primarily during the first post-binding period (protocol II). Anti-CD81 markedly inhibited luciferase activity during protocol II as reported [18,19]. Tamoxifen treatment did not result in clear differences between the protocols and the compound displayed similar activity regardless of the treatment period (Fig. 5b left). As a control, the same experiment was performed using VSVpp. Chloroquine inhibited the early entry step of VSVpp, but anti-CD81 and tamoxifen did not show any inhibition (Fig. 5b right).

Tamoxifen is a lipophilic weak base and inhibits acidification intracellularly [22]. Therefore, we examined whether the inhibition of the endocytosis of HCVpp by tamoxifen was dependent on its function as a weak base. Chloroquine is a weak base and inhibits endosome acidification. The pH sensitivity is considered a good indication of clathrin-dependent endocytosis. Previous reports have indicated that chloroquine inhibited HCVcc and HCVpp infection [14,19]. We adjusted the medium to pH 5.5 and incubated the cells in this acidic medium in the presence or absence of tamoxifen for 2 h post-binding. The acidification of the medium did not affect either the entry of HCVpp or the cell growth (Fig. 5c). Treatment with tamoxifen in the medium with a normal pH (pH 7.1) reduced HCVpp entry, and treatment with the drug in the acidic medium also reduced entry to a similar extent. In contrast, chloroquine treatment in regular medium reduced HCVpp entry, but entry was restored in the acidic medium (Fig. 5c). These results indicate that the inhibitory effect of tamoxifen was not dependent on the function of this compound as a base, unlike the effects of chloroquine.

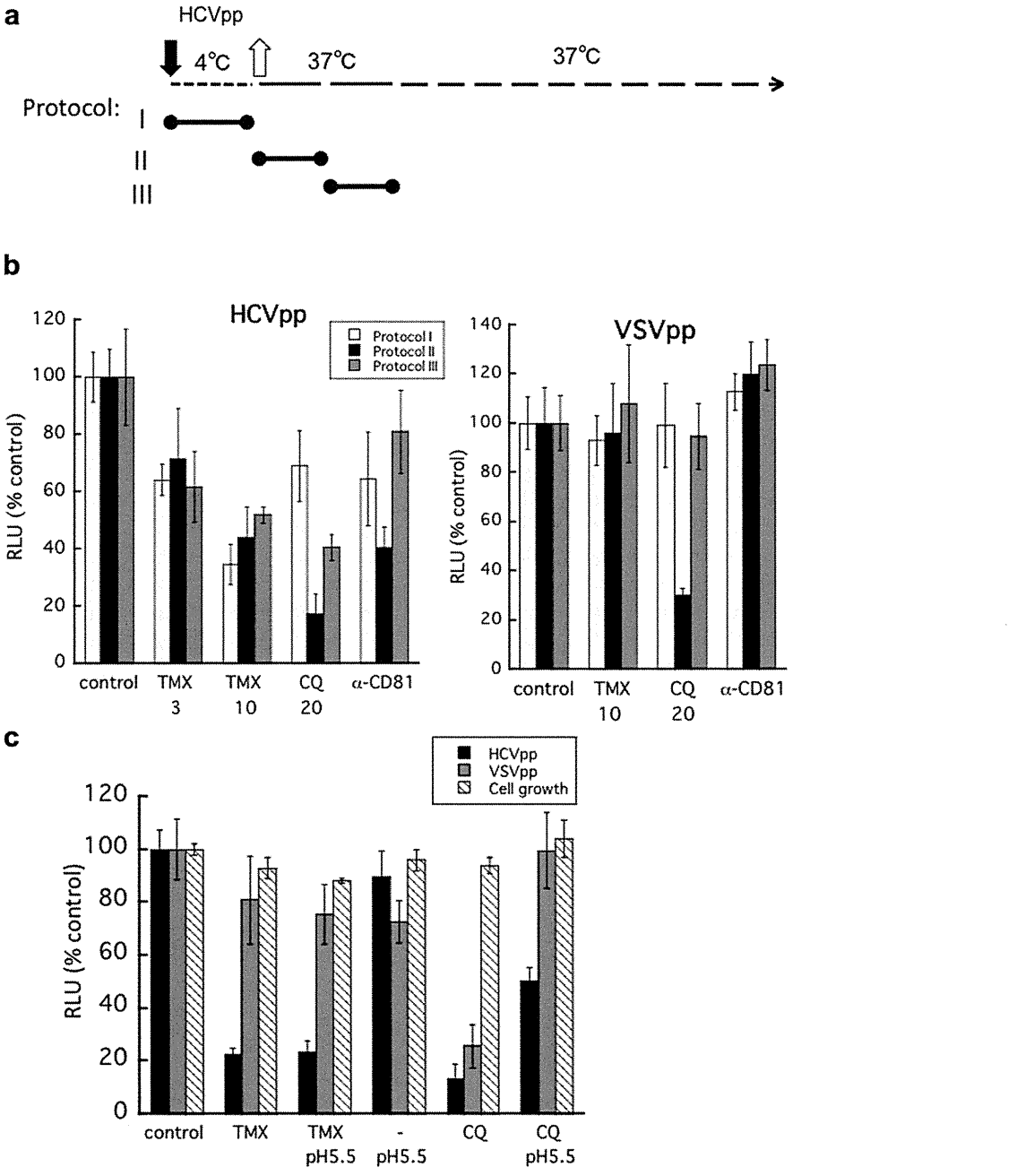

Fig. 5. Effect of tamoxifen on the attachment and endocytosis of HCVpp. a) Experimental design. HCVpp attachment to cells was performed at 4 °C for 1.5 h in the presence or absence of drug. Under these conditions, HCVpp bind to the cells but do not efficiently enter the cells. The inoculum was then removed, and fresh medium was added to the cells. The cells were subsequently incubated at 37 °C. The cells were treated with drug during the binding period at 4 °C (protocol I), during first hour after the shift to 37 °C (protocol II), or 1 h after the shift to 37 °C (protocol III). The drug-containing medium was removed for every treatment, and new medium was supplied to the cells. b) Effects of tamoxifen (TMX) (3 and 10 μM), chloroquine (CQ) (20 μM) and anti-CD81 antibody (20 μg/ml) on HCVpp attachment (protocol I) and post-binding events (protocol II and III) (left). Effects of tamoxifen, chloroquine and anti-CD81 on VSVpp (right). c) Effects of exposure to low pH on the inhibition of HCVpp entry by tamoxifen and chloroquine. The cells were incubated with HCVpp at 4 °C for 1.5 h in the absence of drug. After removing the inoculum, regular (pH 7.1) or acidic medium that was adjusted with HCl to pH 5.5, either with or without drug (tamoxifen, 10 μM, chloroquine, 20 μM), was added to the cells. The cells were subsequently incubated at 37 °C. The drug-containing medium was removed after 2 h of incubation, and the cells were incubated for an additional 3 days with fresh, regular medium. The values are expressed as the percentage of control cells without drug. The data are the averages of three wells and the error bars represent the standard deviation of the mean. One representative experiment of three independent experiments is shown.

4. Discussion

We screened for HCV inhibitors using the JFH-1-Huh 7.5.1 cell culture system and found that tamoxifen and ERα antagonists, but not ERα agonists, inhibited HCV JFH-1 infection. Although there are some reports about the HCV inhibitory effects of tamoxifen and other SERMs, we presented further information about the inhibitory effects of these substances. The time-of-addition experiments (Fig. 2a–c) suggested that these SERMs inhibit the entry and replication

steps in the HCV life cycle. These SERMs, except ICI 182,780, reduced level of HCV genome (genotype 2a) and NS5A (genotypes 1b and 2a) in the subgenomic replicon cells (Fig. 3), which supports the hypothesis that the inhibitory effect of the SERMs occurred during the replication steps. Further we observed that SERMs preferentially reduced extracellular HCV RNA compare to intracellular HCV RNA in the newly (Fig. 2d) and persistently infected cells (Fig. 2e). It suggests that the SERMs also target post replication step(s) in the viral life cycle, such as assembly and release. A low concentration of tamoxifen (0.1 μM) accumulated intracellular HCV RNA (Fig. 2d), which suggests that SERMs target post replication step(s) more efficiently than replication steps. Additionally, these compounds inhibited HCVpp infection (Fig. 4), which supports an inhibitory effect during the entry step. The inhibition of entry was mediated through the inhibition of viral binding to cells and through the inhibition of a post-binding event (Fig. 5b). Taken together, SERMs seemed to target multiple steps of the HCV viral life cycle.

Among the SERMs, ICI 182,780 did not exhibit distinct inhibition of replication in the replicon cells (Fig. 3a and b), although the compound seemed to inhibit entry and replication steps according to the result of time-of-addition experiment (Fig. 2c). The replicon cells are derived from Huh 7 cell. Although viral sensitivity to the SERMs might be dependent on the cell that HCV infect, it remains unclear whether ICI 182,780 inhibits replication step or not. However, the compound affected post replication step in a similar manner to other SERMs (Fig. 2d and e). It is unlikely that ICI 182,780 is an inhibitor with different mechanisms.

The inhibitory effect of tamoxifen on HCV replication has been previously reported by Watashi et al. [23]. They also demonstrated that ICI 182,780 inhibited HCV replication. This effect was discovered using a cell line that harbored a subgenomic replicon (genotype 1b). Additionally, these researchers reported that RNA interference-mediated knockdown of ERα, not ERβ, reduced HCV replication, but the reduction was not related to ERE-mediated transactivation activity. They suggested that ERα interacts with the HCV viral polymerase NS5B and that ERα promotes the participation of NS5B with the HCV replication complex. Using the Huh 7.5.1-JFH-1 screening system, Gastaminza et al. and Chockalingam et al. found that toremifene and raloxifene, respectively, function as HCV inhibitors. Gastaminza et al. [24] reported that toremifene inhibited HCV infection by inhibiting both the entry and release steps of the viral life cycle. Chockalingam et al. [25] determined that raloxifene inhibited the entry and replication steps, as we also observed. Our results are in accordance with these previous reports and other information about the inhibitory effects of SERMs.

Pseudo-particle experiments confirmed that SERMs affected the entry step of HCV viral life cycle (Fig. 4b), although the inhibitory effects were lower compare to those against HCVcc (Fig. 2a–c). The reason for the difference in sensitivity may account for some difference in the two entry systems. Otherwise, in the treatment with the drugs for the first 2 h of HCVcc infection, some amount of the drugs might enter the cell and remain affecting the other steps. The SERMs affected not only genotype 2a but also other genotypes of HCVpp that were examined, suggests that these chemicals have effects on various genotypes of HCV. Although the SERMs appeared to inhibit multiple steps of the HCV life cycle, the primary target step in the viral life cycle might be the entry step. In the time-of-addition experiments, treatment with tamoxifen or raloxifene during the first 2 h was more effective than treatment during the subsequent 2–48 h (Fig. 2a). These SERMs are thought to primarily prevent viral entry and to inhibit post replication step and replication at higher concentrations.

As shown in Fig. 5, an experiment that could discriminate an effect on viral attachment from an effect at the post-binding processes indicated that tamoxifen inhibited both steps. The inhibition of endocytosis by tamoxifen was not rescued by exposure to a low pH. This suggests that the observed inhibition is the result of a mechanism that is independent of the compound's function as a base. HCV entry is a highly complicated process that involves numerous viral and cellular factors. Tamoxifen is thought to target multiple steps that are involved in the attachment and entry steps of the HCV life cycle, which results in high levels of inhibition.

At present, the mechanism of the entry inhibition by SERMs is not clear. It is possible that tamoxifen targets viral molecules, but we have no evidence to support this hypothesis. ERα might be a target molecule because all of the antagonists of ERα that were examined had an inhibitory effect. Watashi et al. indicated that ERα is involved in HCV replication [23]. ERα is thought to be present in the cytoplasm, which is where HCV replicates. However, it is doubtful that ERα is present on the cell surface where viral entry occurs. The addition of 17β-estradiol with tamoxifen did not prevent the inhibitory effect of tamoxifen in the HCVpp experiment (data not shown). This result suggests that tamoxifen does not compete with 17β-estradiol for the target molecules involved in HCV entry. Additionally, a pure ERα antagonist, ICI 182,780, was a less effective inhibitor of the entry step. Based on these results, it is thought that the molecule responsible for HCV entry that is targeted by SERMs is not ERα.

Tamoxifen has various targets other than ERα, such as P-glycoprotein (GPR30), calmodulin, and protein kinase C [26]. GPR30 (G protein-coupled receptor protein 30) is a membrane-associated estrogen receptor that is distinct from the classical ER [27]. Tamoxifen and ICI 182,780 are agonists of GPR30 [28]. We examined the effect of a specific GPR30 agonist, G-1, and a GPR30 antagonist, G-15, on HCVpp infection [29]. G-1 and G-15 did not inhibit HCVpp infection. Conversely, HCVpp infection was observed to increase upon addition of these compounds (data not shown). This result suggested that GPR30 is not involved in the inhibition of HCV entry.

We previously reported that a typical PKC inhibitor, bisindolylmaleimide I (BIM I), inhibited HCV replication [2]. BIM I (10 μM) inhibited both HCVpp and VSVpp infection in a similar manner by approximately 50% (data not shown). This suggests that BIM I has a different mechanism for the

inhibition of entry compared to tamoxifen. PKC is not thought to be involved in the HCV-specific inhibition of entry by SERMs.

There were few reports of HCV entry inhibitors until the development of the cell-culture JFH-1 infection system. It has recently been reported that fluphenazine, trifluoperazine and related chemicals exhibit a strong, dose-dependent inhibition of HCV entry without significantly affecting the entry of VSVpp [24,25]. These compounds are structurally similar to chlorpromazine, which is an inhibitor of the clathrin-coated pit formation that is required for HCV entry [14]. Interestingly, these compounds and the SERMs have a common structural characteristic: planar, multiple aromatic rings with a tertiary amine side chain. Tamoxifen, raloxifene and ERα antagonists all have this structure, but the ERα agonists do not have these structures. Fluphenazine and related chemicals may inhibit HCV entry through a mechanism that is similar to tamoxifen.

In summary, we observed a significant HCV inhibitory effect of various SERMs using the Huh 7.5.1 cell-JFH-1 infection system. Additionally, we demonstrated that SERMs could be useful for the treatment of HCV. Because it takes a great deal of time and money to develop a new drug from a novel chemical compound, it may be easier to use previously developed drugs that can be used for new applications. Tamoxifen, toremifene, and raloxifene are all drugs that have been in use for an extended period of time. In our present *in vitro* study, the effective concentrations for the HCV inhibitory effects of the SERMs were approximately 0.1–10 μM. In the case of tamoxifen, 20 mg per day, administered for 8 weeks resulted in plasma concentrations of approximately 0.5 μM. These concentrations could be sufficient to exert an anti-HCV effect. SERMs should be investigated to determine their efficacy for treating HCV clinically. Further examination of the mechanism of the entry inhibition mediated by SERMs would produce significant new data relevant to the understanding of HCV entry.

Acknowledgments

We thank Drs. Kyoko Murakami, Kenichi Morikawa, Tomoko Date, and Koichi Watashi for helpful advice. We also thank Drs. Françoís-Loïc Cosset (INSERM, France) and Yoshiharu Matsuura (Osaka University, Japan) for generously providing plasmids. This study was supported by a grant-in-aid from the Ministry of Health, Labour and Welfare of Japan.

References

[1] T. Wakita, T. Pietschmann, T. Kato, T. Date, M. Miyamoto, Z. Zhao, K. Murthy, A. Habermann, H.G. Krausslich, M. Mizokami, R. Bartenschlager, T.J. Liang, Production of infectious hepatitis C virus in tissue culture from a cloned viral genome, Nat. Med. 11 (2005) 791–796.

[2] Y. Murakami, K. Noguchi, S. Yamagoe, T. Suzuki, T. Wakita, H. Fukazawa, Identification of bisindolylmaleimides and indolocarbazoles as inhibitors of HCV replication by tube-capture-RT-PCR, Antivir. Res. 83 (2009) 112–117.

[3] T. Kato, T. Date, M. Miyamoto, A. Furusaka, K. Tokushige, M. Mizokami, T. Wakita, Efficient replication of the genotype 2a hepatitis C virus subgenomic replicon, Gastroenterology 125 (2003) 1808–1817.

[4] T. Date, T. Kato, M. Miyamoto, Z. Zhao, K. Yasui, M. Mizokami, T. Wakita, Genotype 2a hepatitis C virus subgenomic replicon can replicate in HepG2 and IMY-N9 cells, J. Biol. Chem. 279 (2004) 22371–22376.

[5] V. Lohmann, F. Korner, J. Koch, U. Herian, L. Theilmann, R. Bartenschlager, Replication of subgenomic hepatitis C virus RNAs in a hepatoma cell line, Science 285 (1999) 110–113.

[6] H. Fukazawa, S. Mizuno, Y. Uehara, A microplate assay for quantitation of anchorage-independent growth of transformed cells, Anal. Biochem. 228 (1995) 83–90.

[7] B. Bartosch, J. Dubuisson, F.L. Cosset, Infectious hepatitis C virus pseudo-particles containing functional E1-E2 envelope protein complexes, J. Exp. Med. 197 (2003) 633–642.

[8] D. Lavillette, A.W. Tarr, C. Voisset, P. Donot, B. Bartosch, C. Bain, A.H. Patel, J. Dubuisson, J.K. Ball, F.L. Cosset, Characterization of host-range and cell entry properties of the major genotypes and subtypes of hepatitis C virus, Hepatology 41 (2005) 265–274.

[9] C.K. Osborne, H. Zhao, S.A. Fuqua, Selective estrogen receptor modulators: structure, function, and clinical use, J. Clin. Oncol. 18 (2000) 3172–3186.

[10] A.E. Wakeling, M. Dukes, J. Bowler, A potent specific pure antiestrogen with clinical potential, Cancer Res. 51 (1991) 3867–3873.

[11] C. Biberger, E. von Angerer, 2-Phenylindoles with sulfur containing side chains. Estrogen receptor affinity, antiestrogenic potency, and antitumor activity, J. Steroid Biochem. Mol. Biol. 58 (1996) 31–43.

[12] J. Sun, Y.R. Huang, W.R. Harrington, S. Sheng, J.A. Katzenellenbogen, B.S. Katzenellenbogen, Antagonists selective for estrogen receptor alpha, Endocrinology 143 (2002) 941–947.

[13] N. Sciaky, J. Presley, C. Smith, K.J. Zaal, N. Cole, J.E. Moreira, M. Terasaki, E. Siggia, J. Lippincott-Schwartz, Golgi tubule traffic and the effects of brefeldin A visualized in living cells, J. Cell Biol. 139 (1997) 1137–1155.

[14] E. Blanchard, S. Belouzard, L. Goueslain, T. Wakita, J. Dubuisson, C. Wychowski, Y. Rouille, Hepatitis C virus entry depends on clathrin-mediated endocytosis, J. Virol. 80 (2006) 6964–6972.

[15] L. Meertens, C. Bertaux, T. Dragic, Hepatitis C virus entry requires a critical postinternalization step and delivery to early endosomes via clathrin-coated vesicles, J. Virol. 80 (2006) 11571–11578.

[16] D.M. Tscherne, C.T. Jones, M.J. Evans, B.D. Lindenbach, J.A. McKeating, C.M. Rice, Time- and temperature-dependent activation of hepatitis C virus for low-pH-triggered entry, J. Virol. 80 (2006) 1734–1741.

[17] A. Op De Beeck, C. Voisset, B. Bartosch, Y. Ciczora, L. Cocquerel, Z. Keck, S. Foung, F.L. Cosset, J. Dubuisson, Characterization of functional hepatitis C virus envelope glycoproteins, J. Virol. 78 (2004) 2994–3002.

[18] B. Bartosch, F.L. Cosset, Cell entry of hepatitis C virus, Virology 348 (2006) 1–12.

[19] E.G. Cormier, R.J. Durso, F. Tsamis, L. Boussemart, C. Manix, W.C. Olson, J.P. Gardner, T. Dragic, L-SIGN (CD209L) and DC-SIGN (CD209) mediate transinfection of liver cells by hepatitis C virus, Proc. Natl. Acad. Sci. U. S. A. 101 (2004) 14067–14072.

[20] E.G. Cormier, F. Tsamis, F. Kajumo, R.J. Durso, J.P. Gardner, T. Dragic, CD81 is an entry coreceptor for hepatitis C virus, Proc. Natl. Acad. Sci. U. S. A. 101 (2004) 7270–7274.

[21] G. Koutsoudakis, A. Kaul, E. Steinmann, S. Kallis, V. Lohmann, T. Pietschmann, R. Bartenschlager, Characterization of the early steps of hepatitis C virus infection by using luciferase reporter viruses, J. Virol. 80 (2006) 5308–5320.

[22] N. Altan, Y. Chen, M. Schindler, S.M. Simon, Tamoxifen inhibits acidification in cells independent of the estrogen receptor, Proc. Natl. Acad. Sci. U. S. A. 96 (1999) 4432–4437.

[23] K. Watashi, D. Inoue, M. Hijikata, K. Goto, H.H. Aly, K. Shimotohno, Anti-hepatitis C virus activity of tamoxifen reveals the functional association of estrogen receptor with viral RNA polymerase NS5B, J. Biol. Chem. 282 (2007) 32765–32772.

[24] P. Gastaminza, C. Whitten-Bauer, F.V. Chisari, Unbiased probing of the entire hepatitis C virus life cycle identifies clinical compounds that target multiple aspects of the infection, Proc. Natl. Acad. Sci. U. S. A. 107 (2010) 291–296.

[25] K. Chockalingam, R.L. Simeon, C.M. Rice, Z. Chen, A cell protection screen reveals potent inhibitors of multiple stages of the hepatitis C virus life cycle, Proc. Natl. Acad. Sci. U. S. A. 107 (2010) 3764–3769.

[26] P. de Medina, G. Favre, M. Poirot, Multiple targeting by the antitumor drug tamoxifen: a structure-activity study, Curr. Med. Chem. Anticancer Agents 4 (2004) 491–508.

[27] E.R. Prossnitz, J.B. Arterburn, L.A. Sklar, GPR30: a G protein-coupled receptor for estrogen, Mol. Cell. Endocrinol. 265–266 (2007) 138–142.

[28] P. Thomas, Y. Pang, E.J. Filardo, J. Dong, Identity of an estrogen membrane receptor coupled to a G protein in human breast cancer cells, Endocrinology 146 (2005) 624–632.

[29] M.K. Dennis, R. Burai, C. Ramesh, W.K. Petrie, S.N. Alcon, T.K. Nayak, C.G. Bologa, A. Leitao, E. Brailoiu, E. Deliu, N.J. Dun, L.A. Sklar, H.J. Hathaway, J.B. Arterburn, T.I. Oprea, E.R. Prossnitz, In vivo effects of a GPR30 antagonist, Nat. Chem. Biol. 5 (2009) 421–427.

Infection and Immunity

Nanogel-Based PspA Intranasal Vaccine Prevents Invasive Disease and Nasal Colonization by Streptococcus pneumoniae

Il Gyu Kong, Ayuko Sato, Yoshikazu Yuki, Tomonori Nochi, Haruko Takahashi, Shinichi Sawada, Mio Mejima, Shiho Kurokawa, Kazunari Okada, Shintaro Sato, David E. Briles, Jun Kunisawa, Yusuke Inoue, Masafumi Yamamoto, Kazunari Akiyoshi and Hiroshi Kiyono

Infect. Immun. **2013, 81(5):1625. DOI: 10.1128/IAI.00240-13.**
Published Ahead of Print 4 March 2013.

IAI
Journals.ASM.org

Nanogel-Based PspA Intranasal Vaccine Prevents Invasive Disease and Nasal Colonization by *Streptococcus pneumoniae*

Il Gyu Kong,[a,b,c] Ayuko Sato,[a,d] Yoshikazu Yuki,[a,d] Tomonori Nochi,[e] Haruko Takahashi,[f] Shinichi Sawada,[f] Mio Mejima,[a] Shiho Kurokawa,[a] Kazunari Okada,[a,d] Shintaro Sato,[a,d] David E. Briles,[g] Jun Kunisawa,[a,d,h,i] Yusuke Inoue,[j] Masafumi Yamamoto,[k] Kazunari Akiyoshi,[f] Hiroshi Kiyono[a,b,d,h]

Division of Mucosal Immunology, Department of Microbiology and Immunology,[a] and International Research and Development Center for Mucosal Vaccines,[h] The Institute of Medical Science, The University of Tokyo, Tokyo, Japan; Graduate School Medicine and Faculty of Medicine, The University of Tokyo, Tokyo, Japan[b]; Department of Otorhinolaryngology, Seoul National University College of Medicine, Seoul, South Korea[c]; Core Research for Evolutional Science and Technology (CREST), Japan Science and Technology Agency, Tokyo, Japan[d]; Division of Infectious Diseases, Center for AIDS Research, University of North Carolina School of Medicine, Chapel Hill, North Carolina, USA[e]; Department of Polymer Chemistry, Kyoto University Graduate School of Engineering, Kyoto, Japan[f]; Department of Microbiology, University of Alabama at Birmingham, Birmingham, Alabama, USA[g]; Laboratory of Vaccine Materials, National Institute of Biomedical Innovation, Osaka, Japan[i]; Department of Diagnostic Radiology, Kitasato University School of Medicine, Kanagawa, Japan[j]; Department of Microbiology and Immunology, Nihon University School of Dentistry at Matsudo, Chiba, Japan[k]

To establish a safer and more effective vaccine against pneumococcal respiratory infections, current knowledge regarding the antigens common among pneumococcal strains and improvements to the system for delivering these antigens across the mucosal barrier must be integrated. We developed a pneumococcal vaccine that combines the advantages of pneumococcal surface protein A (PspA) with a nontoxic intranasal vaccine delivery system based on a nanometer-sized hydrogel (nanogel) consisting of a cationic cholesteryl group-bearing pullulan (cCHP). The efficacy of the nanogel-based PspA nasal vaccine (cCHP-PspA) was tested in murine pneumococcal airway infection models. Intranasal vaccination with cCHP-PspA provided protective immunity against lethal challenge with *Streptococcus pneumoniae* Xen10, reduced colonization and invasion by bacteria in the upper and lower respiratory tracts, and induced systemic and nasal mucosal Th17 responses, high levels of PspA-specific serum immunoglobulin G (IgG), and nasal and bronchial IgA antibody responses. Moreover, there was no sign of PspA delivery by nanogel to either the olfactory bulbs or the central nervous system after intranasal administration. These results demonstrate the effectiveness and safety of the nanogel-based PspA nasal vaccine system as a universal mucosal vaccine against pneumococcal respiratory infection.

The use of polysaccharide-based injectable multivalent pneumococcal conjugate vaccines (PCV7, -10, and -13) has diminished the number of fatal infections due to pneumococci expressing the particular polysaccharides present in the vaccine (1–3). However, *Streptococcus pneumoniae* remains a problematic pathogen (4, 5) because of the large number of different capsular polysaccharides associated with virulent disease in humans. In particular, nonvaccine strains are emerging pathogens that result in morbidity and mortality due to pneumococcal diseases, including pneumonia and meningitis (6–8).

Clinical demand to overcome these problems has prompted the preclinical development of universal serotype-independent pneumococcal vaccines that are based on a surface protein common to all strains. Pneumococcal surface protein A (PspA), a pneumococcal virulence factor (9–13), is genetically variable (14) but highly cross-reactive (9, 10). PspA is commonly expressed by all capsular serotypes of *S. pneumoniae* (15) and is classified into 3 families (family 1, clades 1 and 2; family 2, clades 3 through 5; and family 3, clade 6) according to sequence similarities (14). Given that parenteral immunization with PspA induces cross-reactive neutralizing immune responses in mice (16–18) and humans (19), using PspA as a serotype-independent common antigen for the development of pneumococcal vaccines seems to be an ideal strategy.

Pneumococcal infection is generally preceded by colonization of the upper airway (20, 21). Nasal carriage of pneumococci is the primary source for spread of the infection among humans (22, 23). Therefore, an optimal vaccine strategy to prevent and control the spread of pneumococcal disease would induce protective immunity against both colonization and invasive disease. Several studies have confirmed the efficacy of PspA as a nasal vaccine antigen by coadministering PspA with a mucosal adjuvant such as cholera toxin (CT) or cholera toxin subunit B (CTB) to mice (24–26). The mice subsequently mount antigen-specific immune responses in not only the systemic compartment but also the respiratory mucosal compartment (24, 25, 27), where bacterial colonization occurs (20). PspA-specific secretory immunoglobulin A (sIgA) antibodies induced by intranasal immunization with PspA and an adjuvant (i.e., a plasmid expressing Flt3 ligand cDNA) provide protection against pneumococcal colonization (28). In addition, studies in mice have revealed that this protection is mediated by antigen-specific interleukin 17A (IL-17A)-secret-

Received 20 February 2013 **Accepted** 21 February 2013
Published ahead of print 4 March 2013
Editor: R. P. Morrison
Address correspondence to Hiroshi Kiyono, kiyono@ims.u-tokyo.ac.jp, or Yoshikazu Yuki, yukiy@ims.u-tokyo.ac.jp.
Supplemental material for this article may be found at http://dx.doi.org/10.1128/IAI.00240-13.

doi:10.1128/IAI.00240-13

ing $CD4^+$ T cells induced by intranasal immunization with pneumococcal whole-cell antigen (29, 30).

Therefore, the intranasal vaccination route is an improved route for preventing colonization of the nasal cavity by pneumococci. A leading obstacle to the practical use of nasal vaccine with a protein-based pneumococcal antigen is the need to coadminister a toxin-based mucosal adjuvant (e.g., CT) for effective induction of antigen-specific immune responses (31, 32). However, the use of such toxin-based adjuvants is undesirable in humans, as it carries the concern that the toxin may reach the central nervous system (CNS) or redirect the vaccine antigen into the CNS through the olfactory nerve in the nasal cavity (33, 34). To bypass these concerns, we recently developed a nasal vaccine delivery system based on a non-toxin-based mucosal antigen carrier, a cationic cholesteryl pullulan (cCHP) nanogel (35).

Here we show the efficacy of a nanogel-based nasal pneumococcal vaccine in which PspA is incorporated into a cCHP nanogel (cCHP-PspA). We also characterized the cCHP-PspA-induced PspA-specific Th17 and antibody responses against *S. pneumoniae*. Mice immunized with nasal cCHP-PspA were protected from lethal challenge with *S. pneumoniae* and had fewer pneumococci on their respiratory mucosae. These results suggest that a nontoxic nasal vaccine comprising nanogel-based PspA offers a practical and effective strategy against pneumococcal infection by preventing both nasal colonization and invasive diseases.

MATERIALS AND METHODS

Mice. Female BALB/c mice (aged 6 to 7 weeks) were purchased from SLC (Shizuoka, Japan). All of the mice were housed with *ad libitum* food and water on a standard 12-h–12-h light-dark cycle. All experiments were performed in accordance with the guidelines provided by the Animal Care and Use committees of the University of Tokyo and were approved by the Animal Committee of the Institute of Medical Science of the University of Tokyo.

Recombinant PspA. Recombinant PspA of *S. pneumoniae* Rx1, which belongs to PspA family 1, clade 2 (14), was prepared as described previously, with slight modifications (26). Briefly, a plasmid encoding PspA/Rx1 (pUAB055; amino acids 1 through 302) (GenBank accession no. M74122) was used to transform *Escherichia coli* BL21(DE3) cells. This construct contains amino acids 1 through 302 of the PspA protein from strain Rx1 plus a 6×His tag at the C terminus (26). The sonicated cell supernatant was loaded onto a DEAE-Sepharose column (BD Healthcare, Piscataway, NJ) and a nickel affinity column (Qiagen, Valencia, CA). This was followed by gel filtration on a Sephadex G-100 column (BD Healthcare).

Preparation of cCHP-recombinant PspA complex for intranasal vaccination. A cCHP nanogel (size, ~40 nm) generated from a cationic cholesteryl group-bearing pullulan was used for all experiments. The cCHP-PspA complex for each immunization was prepared by mixing 7.5 μg PspA with cCHP at a 3:1 molecular ratio (volume, 18 μl per mouse) and incubating the mixture for 1 h at 45°C. Before the complex was used in *in vivo* studies, the fluorescence resonance energy transfer (FRET) of fluorescein isothiocyanate (FITC)-PspA and a tetramethyl rhodamine isothiocyanate (TRITC)-cCHP nanogel was measured with a fluorescence spectrometer (model FP-6500; Jasco, Easton, MD) as described previously (37). FRET analyses confirmed that the cCHP nanogel appropriately formed nanoparticles after the incorporation of PspA (see Fig. S1 in the supplemental material). Dynamic light scattering analysis showed that the cCHP nanogel maintained the same nanoscale size (32.8 ± 0.2 nm) even after the incorporation of PspA. Lipopolysaccharide (LPS) contamination of purified PspA and cCHP (<10 endotoxin units/mg protein) was measured with a *Limulus* test (Wako, Osaka, Japan).

Immunization. Once weekly for 3 consecutive weeks, female BALB/c mice were immunized intranasally with cCHP-PspA, PspA plus CT (1 μg; List Biological Laboratory, Campbell, CA), PspA alone, or phosphate-buffered saline (PBS) only. Some experiments included an irrelevant antigen as a control; in these studies, mice were immunized intranasally with a complex of cCHP nanogel and a recombinant nontoxic receptor-binding fragment of *Clostridium botulinum* type A neurotoxin subunit antigen Hc (cCHP-BoHc/A) (35). Serum, nasal wash fluid (NW), and bronchoalveolar lavage fluid (BALF) samples were harvested 1 week after the last immunization. For NWs, 200 μl sterile PBS was flushed through the posterior choanae (38). BALF was harvested by instilling 1 ml of sterile PBS through a blunt needle placed in the trachea (38).

Bacterial strain. We used the kanamycin-resistant pneumococcal strain *S. pneumoniae* Xen10 (Caliper Life Sciences, MA), derived from the wild-type strain A66.1, which expresses PspA of family 1, clades 1 and 2 (39). *S. pneumoniae* Xen10 carries a stable copy of the modified *Photorhabdus luminescens lux* operon at a single integration site on the bacterial chromosome (40). The virulence of *S. pneumoniae* Xen10 is comparable to that of the parent strain (40, 41). For challenge studies, *S. pneumoniae* 3JYP3670, which expresses PspA of family 2, clade 4, was used (10). All of the *S. pneumoniae* strains were grown in brain heart infusion (BHI) broth at 37°C in 5% CO_2.

Pneumococcal infection model. To evaluate the efficacy of intranasal vaccination with cCHP-PspA, mice were challenged 1 week after the last immunization. The cell densities of exponentially growing *S. pneumoniae* Xen10 cultured at 37°C in BHI broth were estimated from the optical density at 600 nm (OD_{600}); cells were pelleted and then diluted with PBS. Lethal (2×10^5 CFU) and sublethal (2×10^4 CFU) challenge doses diluted in 50 μl sterile PBS were administered intranasally to isoflurane-anesthetized mice. Mice were restrained vertically for 5 min to ensure inhalation of the organisms into the trachea. In addition, mice were inoculated intranasally with a lethal challenge dose (5×10^4 CFU) of strain 3JYP3670 in the same way as that for strain Xen10. Nasal passages and lung tissues were homogenized in 500 μl sterile PBS for 1 min, and the numbers of bacterial colonies were determined by plating samples on LB agar plates containing kanamycin (200 μl/ml).

***In vivo* imaging of immunized and challenged mice.** Bioluminescence of bacteria was monitored for 1 min 24, 48, and 72 h after lethal challenge by using an Ivis charge-coupled device (CCD) camera (Xenogen, Alameda, CA). Total photon emission from the entire thorax of each mouse was quantified by using the LivingImage software package (Xenogen). The results are provided as numbers of photons/s/cm^2/sr.

Antibody titer and subclass analysis. Antibody titers were determined by using enzyme-linked immunosorbent assay (ELISA) as described previously, with slight modifications (25). In brief, samples (2-fold serial dilutions) were loaded into individual wells, and the plate was coated with 1 μg/ml recombinant PspA and incubated. Goat anti-mouse IgA, IgG, IgG1, IgG2a, IgG2b, IgG3, and IgM (dilution factor, 1:4,000) conjugated with horseradish peroxidase were used as secondary antibodies. Reactions were visualized by using the TMB microwell peroxidase substrate system (XPL, Gaithersburg, MD). The endpoint titer is expressed as the reciprocal $\log_2$ of the last dilution that gave an OD_{450} that was 0.1 unit greater than that of the negative control.

PspA-specific $CD4^+$ T cell responses. By using anti-CD4 microbeads (Miltenyi Biotec, Sunnyvale, CA) according to the manufacturer's instructions, $CD4^+$ T cells were isolated from the spleens and cervical lymph nodes (CLNs) of mice intranasally immunized with cCHP-PspA, PspA alone, or PBS only. The purified $CD4^+$ T cells were resuspended at 1×10^6 cells/ml in RPMI 1640 (Cellgro, Mediatech, Washington, DC) supplemented with 10 mM HEPES, 50 μM 2-mercaptoethanol, 100 U/ml penicillin, 100 μl/ml streptomycin, and 10% fetal calf serum and then cocultured with irradiated (2,000 rad) splenic antigen-presenting cells (2×10^6 cells/ml) from naïve BALB/c mice for 5 days at 37°C in 5% CO_2 in the presence of 1 μg/ml PspA. Cytokine levels in $CD4^+$ T cell culture supernatants were determined by using cytokine-specific DuoSet ELISA kits

(R&D Systems, Minneapolis, MN) according to the manufacturer's instructions.

Radioisotope counting assay. To trace the distribution of PspA after intranasal immunization, PspA was labeled with indium chloride (Nihon Medi-Physics, Tokyo, Japan) anhydride (Dojindo, Kumamoto, Japan) via N-terminal and ε-Lys amino groups, using diethylenetriaminepentaacetic acid as described previously (42). ^{111}In-labeled PspA was administered alone or as a complex with cCHP nanogel. The radioisotope counts in the nasal passage, olfactory bulbs, and brain 10 min and 1, 6, 12, 24, and 48 h after instillation were estimated with a γ-counter (Wizard model 1480; PerkinElmer, Waltham, MA). The results are provided as standardized uptake values (SUVs), calculated as radioisotope counts (cpm) per gram of tissue divided by the ratio of the injected dose (1×10^6 cpm) to body weight (in grams).

Flow cytometric analysis. Mice were immunized intranasally with FITC-PspA in cCHP nanogel, FITC-PspA alone, or PBS only; 6 h later, mononuclear cells were prepared from the nasal passages of each group by mechanical dissociation through 70-μm nylon mesh, as described previously (38, 43). Isolated cells were stained with phycoerythrin (PE)-Cy7-conjugated anti-CD11c (BD Bioscience) and analyzed by flow cytometry. The percentage of PspA$^+$ cells in the CD11c$^+$ fractions was calculated for each experimental group.

Data analysis. Data are expressed as means ± standard deviations (SD). Statistical analysis for most comparisons among groups was performed with Tukey's *t* test; differences were considered statistically significant when the *P* value was <0.05. For survival data, the Fisher exact test was used to compare the numbers of alive versus dead mice in the cCHP-PspA, PspA-CT, and PBS-only groups with those in the PspA-only group.

RESULTS

Intranasal vaccination with cCHP-PspA induces protective immunity against lethal challenge with *S. pneumoniae*. To evaluate whether intranasal cCHP-PspA vaccination induces protective immunity against pneumococcal challenge, we vaccinated mice with cCHP-PspA, PspA-CT, PspA alone, or PBS only. One week after the last immunization, we lethally challenged vaccinated mice with the virulent strain *S. pneumoniae* Xen10 (2×10^5 CFU), which is *S. pneumoniae* A66.1 rendered bioluminescent by the integration of a modified *lux* operon into its chromosome (40). The PspA expression level of strain Xen10 was confirmed to be comparable to that of the parent strain (see Fig. S2 in the supplemental material). We then evaluated survival rates after lethal challenge over a 2-week period. The survival rate of the cCHP-PspA-vaccinated group was 100%, as was that for PspA-CT-vaccinated mice (Fig. 1). In contrast, most of the mice intranasally immunized with PspA alone (survival rate, 0%) or with PBS (20% survival) died within 8 days of challenge with *S. pneumoniae* Xen10 (Fig. 1). The survival rates of the groups immunized with cCHP-PspA or PspA-CT were higher and were statistically significant compared to that of the group immunized with PspA alone ($P < 0.01$). The results from the PspA-only and PBS-only groups did not differ ($P > 0.05$). In addition, immunization with the irrelevant antigen BoHc/A incorporated into cCHP (cCHP-BoHc/A) (35) did not protect mice from challenge with *S. pneumoniae* Xen10 (see Fig. S3). Because PspA family 2 (clades 3 through 5) and family 1 (clades 1 and 2) constitute 94 to 99% of clinical isolates of pneumococci (14, 44–49), we also challenged mice with the strain 3JYP3670, which expresses PspA belonging to clade 4 of family 2 (10). Unlike mice inoculated with cCHP-BoHc/A, PspA alone, or PBS only, mice nasally immunized with cCHP-PspA were protected from lethal challenge with 3JYP3670 (PspA of clade 4) (10), as was the case with Xen10 expressing PspA of clades 1 and 2 (see Fig. S4).

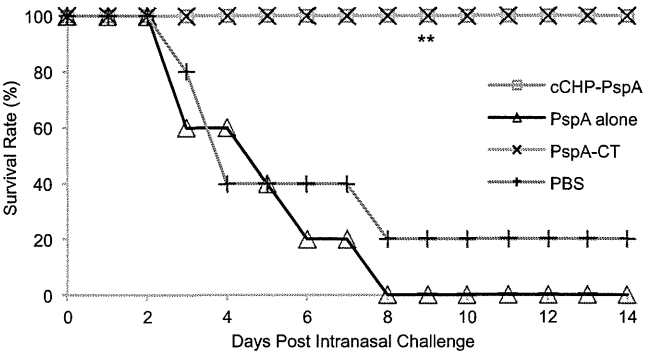

FIG 1 Intranasal vaccination with cCHP-PspA induced protective immunity against pneumococci. One week after the final immunization, mice were challenged with *S. pneumoniae* Xen10 (2×10^5 CFU/mouse), and survival was monitored. Data are representative of three independent experiments, and each group consisted of 5 mice. *P* values were calculated by using the Fisher exact test to compare the numbers of alive versus dead mice in each group with the result obtained for the PspA-only group. **, $P < 0.01$ compared with the group immunized with PspA alone. Abbreviations: cCHP, cationic cholesteryl group-bearing pullulan; CT, cholera toxin; PspA, pneumococcal surface protein A.

Intranasal vaccination with cCHP-PspA enhances bacterial clearance from BALF and the lung. To assess whether intranasal immunization with cCHP-PspA prevented pulmonary infection with pneumococci, we performed *in vivo* bioluminescence imaging of *S. pneumoniae* Xen10 after lethal challenge (2×10^5 CFU) of mice intranasally vaccinated with cCHP-PspA, PspA alone, or PBS. The lungs of mice immunized with PspA alone or with PBS only (control group) showed high-intensity photon signals in a pattern consistent with that of full-blown lung infection (Fig. 2A). In contrast, the lungs of mice immunized with cCHP-PspA lacked bioluminescence, indicating the absence of pulmonary infection. Forty-eight and 72 h after infection, photon counts of the cCHP-PspA-vaccinated group were significantly lower than those of the other two groups (Fig. 2B).

To investigate whether intranasal immunization with cCHP-PspA hastened bacterial clearance from the lung, we counted the bacteria in the BALF and lung tissues of mice intranasally vaccinated with cCHP-PspA, PspA alone, or PBS and sublethally challenged with *S. pneumoniae* Xen10 (2×10^4 CFU). Three hours after challenge, bacterial numbers in BALF (Fig. 2C) and lung tissue (Fig. 2D) did not differ among the three vaccination groups. However, 24 h after challenge, the bacterial counts in the BALF and lung homogenates from the cCHP-PspA-vaccinated groups were significantly lower (about 100-fold) than those for the mice immunized with PspA alone or PBS only (Fig. 2C and D).

Intranasal vaccination with cCHP-PspA reduces bacterial colonization in the nasal cavity. We next examined whether intranasal cCHP-PspA immunization affected nasal carriage of pneumococci in mice challenged with *S. pneumoniae* Xen10. Three days after challenge, bacterial numbers in NWs (Fig. 3A) and nasal passages (Fig. 3B) of mice immunized with the cCHP-PspA nasal vaccine were decreased significantly (approximately 100-fold) compared to those for the two control groups.

Intranasal vaccination with cCHP-PspA induces strong Th17 and Th2 responses. We then examined the type of immune

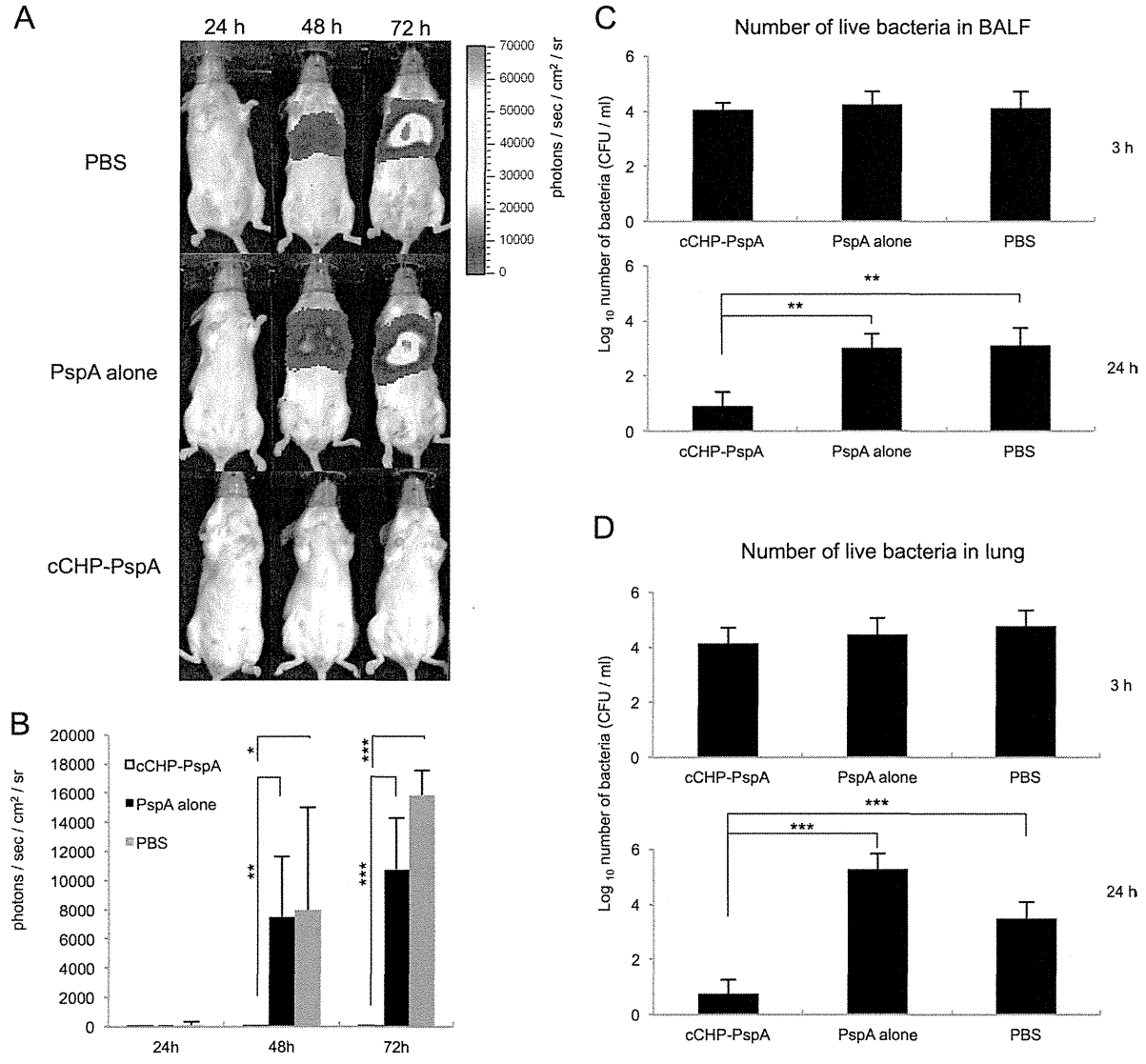

FIG 2 *In vivo* imaging revealed no sign of pneumococcal infection in the lungs of mice immunized intranasally with cCHP-PspA; these mice also showed enhanced bacterial clearance from the BALF and lung. Images (A) and average photon counts (B) show bioluminescence due to *S. pneumoniae* Xen10 in each group of mice infected intranasally with *S. pneumoniae* Xen10 (2×10^5 CFU/mouse) and imaged 24, 48, and 72 h after infection. (C and D) One week after the final immunization, mice were challenged with a sublethal dose (2×10^4 CFU/mouse) of *S. pneumoniae* Xen10. BALF and lung tissues were collected, and the numbers of *S. pneumoniae* Xen10 organisms 3 and 24 h after challenge were determined. Data are representative of three independent experiments, and each group consisted of 5 mice. *, $P < 0.05$; **, $P < 0.01$; ***, $P < 0.001$. Abbreviations: BALF, bronchoalveolar lavage fluid; cCHP, cationic cholesteryl-group-bearing pullulan; PspA, pneumococcal surface protein A.

responses elicited by intranasal cCHP-PspA vaccination. Compared with PspA alone or PBS, cCHP-PspA induced higher levels of IL-17 in $CD4^+$ T cells from the spleen, CLNs, and nasal passages (Fig. 4A). The cCHP-PspA-vaccinated group produced high levels of IL-4 and IL-13, the hallmark cytokines of a Th2-type immune response, but only scant amounts of gamma interferon (Fig. 4B to D). These results show the potential of a cCHP-PspA nasal vaccine as an advanced pneumococcal vaccine that can induce a Th17 response together with a Th2-type immune response.

Intranasal vaccination with cCHP-PspA induces high levels of systemic antibodies. To address whether intranasal administration of cCHP-PspA induced PspA-specific antibody responses, we examined the serum titers of PspA-specific antibodies. PspA-specific IgG responses in the systemic compartment were significantly higher in mice immunized with intranasal cCHP-PspA than in those given PspA only (Fig. 5A). Unlike the predominant IgG response, IgM and IgA titers in the serum samples were very low (Fig. 5A).

Intranasal immunization with cCHP-PspA induced primarily IgG1 antibodies, followed by IgG2b antibodies (Fig. 5B). This pattern indicated skewing toward a Th2-type response and was consistent with the cytokine profiles of the culture supernatants from antigen-stimulated $CD4^+$ T cells prepared from the same mice (Fig. 4B and C).

Intranasal vaccination with cCHP-PspA induces high levels of mucosal antigen-specific sIgA antibodies. We next examined whether vaccinated mice also produced mucosal antigen-specific Ig responses. Intranasal vaccination with cCHP-PspA induced

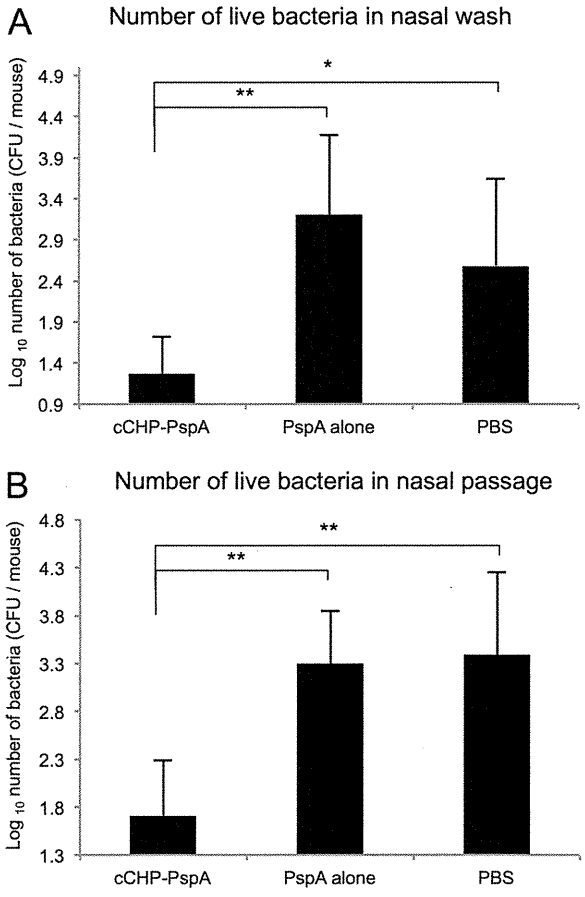

FIG 3 Intranasal vaccination with cCHP-PspA reduced bacterial colonization of the nasal cavity. One week after the final immunization, mice were challenged with a sublethal dose (2×10^4 CFU/mouse) of *Streptococcus pneumoniae* Xen10. Nasal washes and tissues were collected, and the numbers of *S. pneumoniae* Xen10 3 days after infection were determined. Data are representative of three independent experiments, and each group consisted of 5 mice. *, $P < 0.05$; **, $P < 0.01$. Abbreviations: cCHP, cationic cholesteryl group-bearing pullulan; PspA, pneumococcal surface protein A.

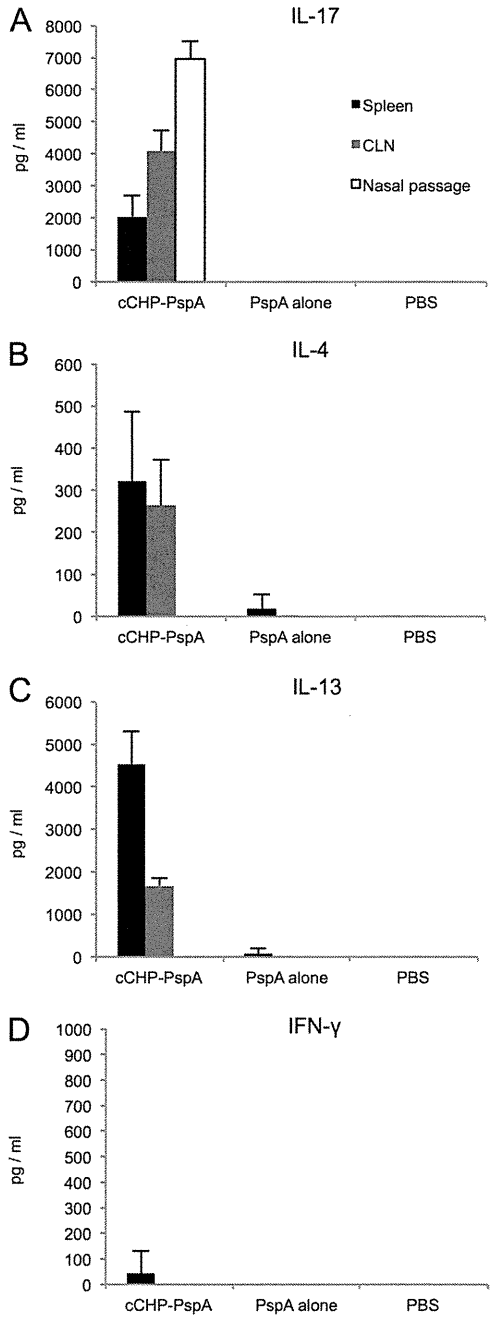

FIG 4 $CD4^+$ T cells from cCHP-PspA-immunized mice produce Th17- and Th2-type immune responses. Cytokines produced by $CD4^+$ T cells isolated from the spleens, cervical lymph nodes, and nasal passages of mice immunized with cCHP-PspA, PspA alone, or PBS only were analyzed. Data are representative of five independent experiments, and each group consisted of 5 mice. Abbreviations: cCHP, cationic cholesteryl-group-bearing pullulan; CLN, cervical lymph node; IFN-γ, gamma interferon; IL, interleukin; PspA, pneumococcal surface protein A.

PspA-specific mucosal IgA antibodies in the nasal secretions (Fig. 6A). In addition, BALF samples from mice intranasally vaccinated with cCHP-PspA contained PspA-specific IgA antibodies (Fig. 6B), and PspA-specific IgG antibodies were detected at high titers in both the NWs and BALF of mice intranasally immunized with cCHP-PspA (Fig. 6C and D). The nasal and BALF antigen-specific IgGs induced by intranasal immunization with cCHP-PspA were primarily of the IgG1 and IgG2b subclasses (Fig. 6E and F), similar to the Ig responses in the systemic compartment (Fig. 5B). Taken together, these results further support the benefit of cCHP-based nanogel as an effective nasal vaccine delivery vehicle for the induction of PspA-specific systemic and mucosal antibody responses against *S. pneumoniae*.

cCHP delivers PspA to dendritic cells (DCs) without CNS accumulation of PspA. The potential for antigen deposition and accumulation in the CNS through the olfactory fossa is one of the great concerns surrounding the use of nasal vaccines (33, 34, 50). To address this important concern, we instilled ^{111}In-labeled PspA alone or in complex with cCHP into the nasal cavities of mice. Beginning 6 h after administration, the nasal passages of mice treated with ^{111}In-labeled cCHP-PspA had higher SUVs than did those of mice treated with ^{111}In-labeled PspA alone, but there was no accumulation of ^{111}In-labeled PspA in the olfactory bulbs or brain throughout the 48-h observation period (Fig. 7A).

The cCHP vaccine delivery system enabled prolonged antigen exposure at the nasal epithelium, allowing continuous antigen

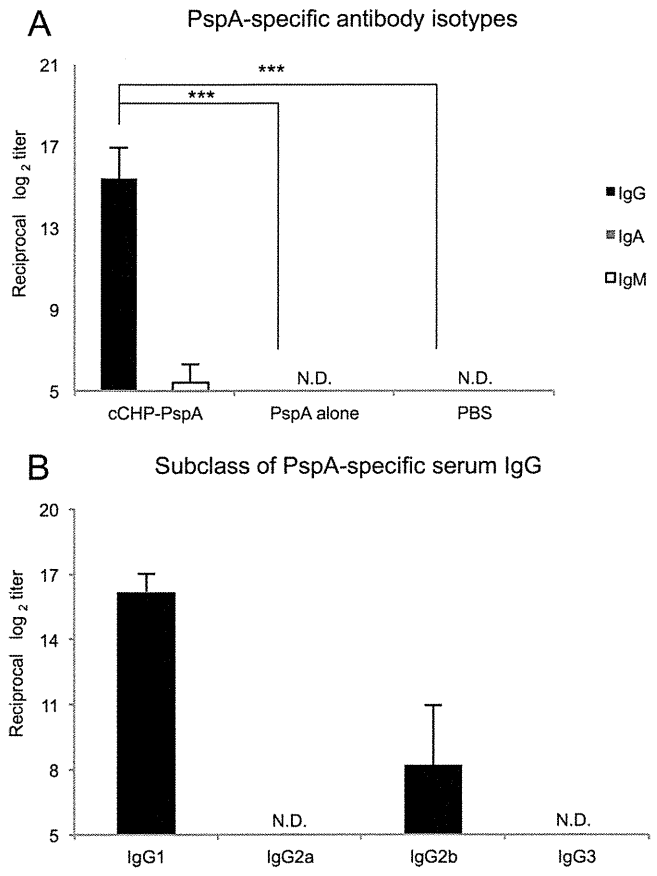

FIG 5 Intranasal vaccination with cCHP-PspA induced high levels of systemic antibodies. The data show the PspA-specific serum IgG level (A) and subclass analysis for IgG1, IgG2a, IgG2b, and IgG3 (B) for each immunized group (cCHP-PspA, PspA alone, or PBS only). Titers of PspA-specific IgG in sera were measured on day 7 after final immunization. Data are representative of three independent experiments, and each group consisted of 5 mice. N.D., not detected by ELISA with samples diluted 1:32. ***, $P < 0.001$. Abbreviations: cCHP, cationic cholesteryl group-bearing pullulan; Ig, immunoglobulin; PspA, pneumococcal surface protein A.

uptake by nasal DCs located in the epithelial layer and lamina propria of the nasal passages for the initiation of antigen-specific immune responses. Whereas 17.8% of the DCs located in the nasal passages had taken up PspA in the mice intranasally immunized with cCHP-PspA, only 0.7% of nasal DCs contained PspA antigen in mice that had been immunized intranasally with PspA alone (Fig. 7B). These results further support the concept that the cCHP-PspA vaccine formulation is an attractive inhalant delivery vehicle that effectively delivers and sustains antigen at the nasal epithelium for continuous antigen uptake by DCs without antigen deposition in the CNS.

DISCUSSION

We showed that cCHP-PspA-vaccinated mice survived a lethal challenge with *S. pneumoniae* (Fig. 1; see Fig. S4 in the supplemental material), whereas mice vaccinated with cCHP complexed with an irrelevant antigen (BoHc/A) did not (see Fig. S3 and S4). Importantly, compared with those of mice inoculated with control constructs, the respiratory tracts of mice immunized with intranasal cCHP-PspA had less colonization and invasion by pneumococcal organisms (Fig. 2 and 3). Intranasal administration of cCHP-PspA resulted in enhanced PspA-specific Th17 responses (Fig. 4A) and mucosal IgA and systemic IgG antibody responses (Fig. 5 and 6), all of which are involved in establishing protective immunity against pneumococci (10, 28–30). To our knowledge, the current study is the first to show the efficacy of a nasal vaccine not only for inducing protective immune responses but also for preventing nasal colonization by use of a single protein antigen (PspA) without adding any biologically active adjuvant.

The precise mechanisms underlying the efficacy of cCHP-PspA as a nasal vaccine against *S. pneumoniae* lung infection remain to be elucidated. However, we speculate that serum and BALF IgGs, the main isotype of antibody induced by the cCHP-PspA nasal vaccine in the lower respiratory compartment (Fig. 5A and 6D), play key roles in survival against lethal challenge with *S. pneumoniae*, given that antibody titers of PspA-specific IgA in the BALF were low (Fig. 6B) and therefore might contribute only minimally to protection against invasive diseases. This hypothesis is supported by the results of a previous study (28) in which $IgA^{-/-}$ mice immunized with intranasal PspA-adjuvant (i.e., a plasmid expressing Flt3 ligand cDNA) mounted a protective immune response against lethal challenge with *S. pneumoniae*. Our current study shows that the cCHP-PspA nasal vaccine effectively induced antigen-specific sIgA antibodies in the upper airways (Fig. 6A). Immunization of $IgA^{-/-}$ mice with intranasal PspA-adjuvant did not prevent pneumococcal colonization of the nasal cavity (28). In light of the findings of the previous study (28) and our current one, serum antigen-specific IgG antibodies are crucial to preventing invasive disease associated with clinical signs, whereas antigen-specific sIgA antibodies are essential for preventing colonization of the upper respiratory tract by *S. pneumoniae*.

In addition to the essential role of sIgA in protection from nasopharyngeal colonization by pneumococci, IL-17A-producing $CD4^+$ T cells play an important role in preventing pneumococcal nasal colonization in mice immunized with intranasal pneumococcal whole-cell antigen (29, 30). Recent studies have found that IL-17 promotes multiple aspects of humoral immunity by enhancing B cell proliferation and isotype switching (51), B cell recruitment to the respiratory mucosa, and expression of the polymeric immunoglobulin receptor on the airway epithelium (52). In the current study, we found that intranasal immunization with cCHP-PspA generated Th17 cells in the nasal passages, draining lymph nodes, and systemic compartment (Fig. 4A). Therefore, our findings suggest that intranasal immunization with cCHP-PspA induces both humoral and cellular immune responses, which are required for protective immunity against pneumococcal colonization and invasive disease. In addition to their essential role in antipneumococcal immunity (29, 30), Th17 responses are a hallmark of autoimmunity (53). Therefore, future studies should carefully examine whether the Th17 responses induced by intranasal immunization with cCHP-PspA are associated with any adverse effects.

As one might expect, the protective immunity induced by nasal cCHP-PspA was not observed when an irrelevant antigen, BoHc/A, was incorporated into cCHP (cCHP-BoHc/A) (35) and used as a nasal vaccine (see Fig. S3 and S4 in the supplemental material). Moreover, mice immunized intranasally with cCHP-PspA (PspA of clades 1 and 2) were protected against challenge with pneumococcal strain 3JYP3670, which expresses PspA of clade 4 (10), whereas mice immunized with cCHP-BoHc/A, PspA